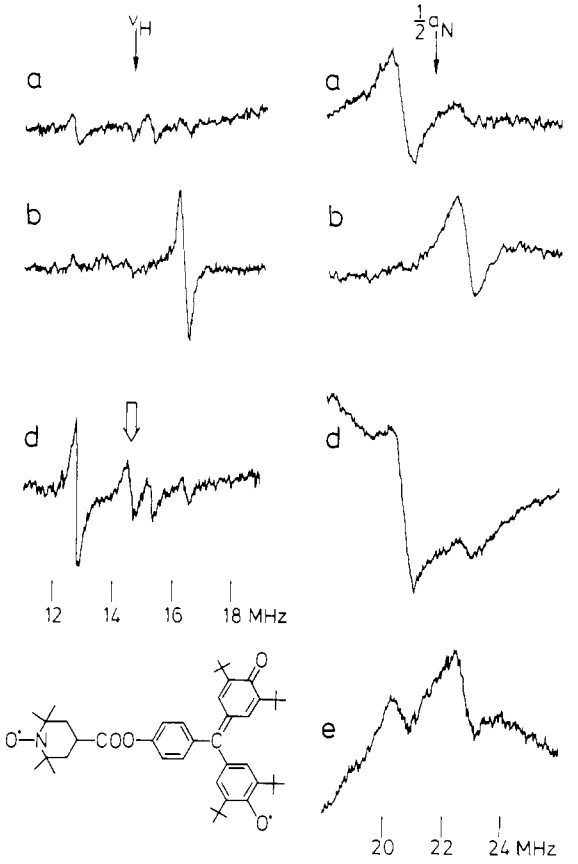

Figure 9. ^1H (left) and ^{14}N (right) ENDOR spectra of biradical **10b** at different off-center field settings (cf. Figure 4, center). Note the appearance of an ENDOR line at the free proton frequency (see arrow in spectrum d, left).

intense for the field setting d; see Figure 9. According to the arguments presented in the Theory, this "free proton frequency line" presumably arises from NMR transitions of protons with small coupling constants, e.g., *tert*-butyl protons, within the $M_S = 0$ manifold.

Finally, it should be mentioned that ENDOR spectra could also be obtained from biradical **16b**. The results are analogous to those for **10b**; see Table III. Attempts to record fluid solution ENDOR spectra of biradicals with larger zero-field splittings, e.g., **9b**, however, failed because of the strong relaxation processes caused by the electron–electron dipolar interaction. Thus it can be stated that under the experimental conditions used in this investigation (e.g., magnitude of microwave and radiofrequency power), successful fluid solution ENDOR on biradicals can only be performed for D values $< \sim 100$ MHz.

Conclusions

It has been shown that mixed galvinoxyl/nitroxide biradicals are suitable model compounds for the study of electron–electron spin exchange between different types of radicals. The magnitude of the exchange integral J relative to that of the nitrogen hyperfine coupling constant a^N varies from $|J| < |a^N|$ to $|J| \gg |a^N|$, depending on the length of the connecting bridge. Whereas the splittings observed in the ESR spectra do not represent the hyperfine coupling constants when the exchange integral has about the same magnitude, the ENDOR technique allows *direct measurements* of these coupling constants. Moreover, by means of ENDOR experiments it is possible to deduce the *sign of the exchange integral* relative to those of the hyperfine couplings. This is remarkable, since the sign determination from ESR is restricted to favorable cases and requires an elaborate analysis[15,16] and susceptibility measurements are not applicable if the exchange integral is small (i.e., $|J| \ll kT$). Actually, in the present paper the signs of the exchange integral could be determined for three of the mixed galvinoxyl/nitroxide biradicals and were found to be negative. Hence in these systems the triplet state unambiguously is the ground state. This is in contrast to several symmetrical bis(nitroxides) for which a positive sign of J was deduced.[15,16]

Finally, it should be pointed out that the present investigation opens an interesting aspect for the "absolute" sign determination of hyperfine coupling constants. It might be possible to prepare a weakly coupled biradical from the radical under study by means of the spin-labeling technique. An ENDOR experiment will then allow the determination of the signs relative to those of the spin label assumed to be known.

Acknowledgment. We are indebted to E. Brinkhaus, Freie Universität Berlin, for performing very careful ESR measurements. This work was supported by the Deutsche Forschungsgemeinschaft (Normalverfahren) and by the Fonds der Chemischen Industrie, which is gratefully acknowledged.

Registry No. 1b, 14635-89-3; **2a**, 81790-03-6; **3a**, 81769-81-5; **4a**, 81769-82-6; **5a**, 81769-83-7; **6**, 2896-70-0; **7**, 2226-96-2; **8**, 54416-73-8; **9a**, 81769-84-8; **9b**, 81790-04-7; **10a**, 81769-85-9; **10b**, 81769-86-0; **11a**, 81769-87-1; **11b**, 81769-88-2; **12**, 2154-32-7; **13a**, 81769-89-3; **13b**, 81769-90-6; **14a**, 81769-91-7; **14b**, 81769-92-8; **15a**, 81769-93-9; **15b**, 81769-94-0; **16a**, 81769-95-1; **16b**, 81769-96-2; **17a**, 81769-97-3; **17b**, 81769-98-4.

Perpendicular and Parallel Acetylene Complexes

David M. Hoffman, Roald Hoffmann,* and C. Richard Fisel

Contribution from the Department of Chemistry, Cornell University, Ithaca, New York 14853.
Received September 21, 1981

Abstract: A molecular orbital analysis of $L_3M(acetylene)ML_3$ complexes serves as an introduction to a general study of perpendicular- and parallel-bonded dinuclear transition-metal acetylene complexes. The two alternative geometries have different electronic requirements—the perpendicular acetylene has four frontier orbitals above a d^6–d^6 block and a metal–metal bond, the parallel-bonded acetylene has five such orbitals. Parallel and perpendicular acetylenes coexist for the same metal d-electron count, yet their interconversion by a simple twisting is not a likely process. If not forbidden by a level crossing, twisting generates instabilities that are relieved by a change in the coordination geometry of the metal. Isolobal analogies relating the acetylene complexes to tetrahedrane, olefins, and cyclobutadiene are a useful guide to their transformations.

As one examines dinuclear transition-metal complexes with bridging acetylene, $L_nM(acetylene)ML_n$, one is first struck by the structural diversity of the L_nMML_n moiety. Yet there is a clear partitioning, a dichotomy of all the known complexes; the acetylene is invariably situated nearly parallel, **1a**, or nearly perpendicular, **1b**, to the M–M vector. In Table I is given a partial listing, with

0002-7863/82/1504-3858$01.25/0 © 1982 American Chemical Society

I

some selected structural data, of the acetylene complexes whose solid-state structures have been determined.

(1) Gilmore, C. J.; Woodward, P. *J. Chem. Soc., Chem. Commun.* **1971**, 1233–1234.
(2) Koie, Y.; Shinoda, S.; Saito, Y.; Fitzgerald, B. J.; Pierpont, C. G. *Inorg. Chem.* **1980**, *19*, 770–773.
(3) Jarvis, J. A. J.; Johnson, A.; Puddephatt, R. J. *J. Chem. Soc., Chem. Commun.* **1973**, 373–374.
(4) Blach, A. L.; Lee, C.-L.; Lindsay, C. H.; Olmstead, M. M. *J. Organomet. Chem.* **1979**, *177*, C22–C26.
(5) Cowie, M.; Dickson, R. S. *Inorg. Chem.* **1981**, *20*, 2682–2688.
(6) Cowie, M.; Southern, T. G. *J. Organomet. Chem.* **1980**, *193*, C46–C50.
(7) (a) Wong, Y. S.; Paik, H. N.; Chieh, P. C.; Carty, A. J. *J. Chem. Soc., Chem. Commun.* **1975**, 309–310. (b) Carty, A. J.; Mott, G. N.; Taylor, N. J. *J. Organomet. Chem.* **1981**, *212*, C54–C58. (c) Carty, A. J.; Taylor, N. J.; Smith, W. F. *J. Chem. Soc., Chem. Commun.* **1978**, 1017–1019.
(8) (a) Bennett, M. J.; Graham, W. A. G.; Stewart, R. P., Jr.; Tuggle, R. M. *Inorg. Chem.* **1973**, *12*, 2944–2949. (b) Dickson, R. S.; Johnson, S. H.; Kirsch, H. P.; Lloyd, D. J. *Acta Crystallogr., Sect. B* **1977**, *B33*, 2057–2061. Dickson, R. S.; Mok, C.; Pain, G. *J. Organomet. Chem.* **1979**, *166*, 385–402. (c) Jarvis, A. C.; Kemmitt, R. D. W.; Russell, D. R.; Tucker, P. A. *Ibid.* **1978**, *159*, 341–355. (d) Rausch, M. D.; Gastinger, R. G.; Gardner, S. A.; Brown, R. K.; Wood, J. S. *J. Am. Chem. Soc.* **1977**, *99*, 7870–7876.
(9) Davidson, J. L.; Harrison, W.; Sharp, D. W. A.; Sim, G. A. *J. Organomet. Chem.* **1972**, *46*, C47–C49.
(10) Staal, L. H.; Polm, L. H.; Vrieze, K. *J. Organomet. Chem.* **1980**, *199*, C13–C16. Staal, L. H.; van Koten, G.; Vrieze, K.; Ploeger, F.; Stam, C. H. *Inorg. Chem.* **1981**, *20*, 1830–1835.
(11) (a) Clemens, J.; Green, M.; Kuo, M.-C.; Fritchie, C. J.; Mague, J. T.; Stone, F. G. A. *J. Chem. Soc., Chem. Commun.* **1972**, 53–54. (b) Smart, L. E.; Browning, J.; Green, M.; Laguna, A.; Spencer, J. L.; Stone, F. G. A. *J. Chem. Soc., Dalton Trans.* **1977**, 1777–1785.
(12) (a) Day, V. W.; Abdel-Meguid, S. S.; Dabestani, S.; Thomas, M. G.; Pretzer, W. R.; Muetterties, E. L. *J. Am. Chem. Soc.* **1976**, *98*, 8289–8291. Muetterties, E. L.; Pretzer, W. R.; Thomas, M. G.; Beier, B. F.; Thorn, D. L.; Day, V. W.; Anderson, A. B. *Ibid.* **1978**, *100*, 2090–2096. (b) Boag, N. M.; Green, M.; Howard, J. A. K.; Stone, F. G. A.; Wadepohl, H. *J. Chem. Soc., Dalton Trans.* **1980**, 862–872. (c) Green, M.; Grove, D. M.; Howard, J. A. K.; Spencer, J. L.; Stone, F. G. A. *J. Chem. Soc., Chem. Commun.* **1976**, 759–760.
(13) (a) Cotton, F. A.; Jamerson, J. D.; Stults, B. R. *J. Am. Chem. Soc.* **1976**, *98*, 1774–1779. (b) Sly, W. G. *Ibid.* **1959**, *81*, 18–20. (c) Bonnett, J.-J.; Mathieu, R. *Inorg. Chem.* **1978**, *17*, 1973–1976. (d) Bianchini, C.; Dapporto, P.; Meli, A. *J. Organomet. Chem.* **1979**, *174*, 205–212. (e) Bird, P. H.; Fraser, A. R.; Hall, D. N. *Inorg. Chem.* **1977**, *16*, 1923–1931. (f) Bailey, N. A.; Churchill, M. R.; Hunt, R.; Mason, R.; Wilkinson, G. *Proc. Chem. Soc. (London)* **1964**, 401. Bailey, N. A.; Mason, R. *J. Chem. Soc. A* **1968**, 1293–1299. (g) Bennett, M. A.; Johnson, R. N.; Robertson, G. B.; Turney, T. W.; Whimp, P. O. *J. Am. Chem. Soc.* **1972**, *94*, 6540–6541; *Inorg. Chem.* **1976**, *15*, 97–107. (h) Angoletta, M.; Bellon, P. L.; Demartin, F.; Sansoni, M. *J. Organomet. Chem.* **1981**, *208*, C12–C14. (i) Freeland, B. H.; Hux, J. E.; Payne, N. C.; Tyers, K. G. *Inorg. Chem.* **1980**, *19*, 693–696. (j) Wang, Y.; Coppens, P. *Ibid.* **1976**, *15*, 1122–1127. (k) Mills, O. S.; Shaw, B. W. *J. Organomet. Chem.* **1968**, *11*, 595–699. (l) Restiva, R. J.; Ferguson, G.; Ng, T. W.; Carty, A. J. *Inorg. Chem.* **1977**, *16*, 172–176. (m) Ban, E.; Cheng, P.-T.; Jack, T.; Nyberg, S. C.; Powell, J. *J. Chem. Soc., Chem. Commun.* **1973**, 368–369; Jack, T. R.; May, C. J.; Powell, J. *J. Am. Chem. Soc.* **1977**, *99*, 4707–4716.
(14) Dickson, R. S.; Pain, G. N.; Mackay, M. F. *Acta Crystallogr., Sect. B* **1979**, *B35*, 2321–2325.
(15) Cotton, F. A.; Hall, W. T. *Inorg. Chem.* **1980**, *19*, 2354–2356.
(16) Chisholm, M. H.; Huffman, J. C.; Rothwell, I. P., submitted for publication.
(17) Fischer, E. O.; Ruhs, A.; Friedrich, P.; Huttner, G. *Angew. Chem., Int. Ed. Engl.* **1977**, *16*, 465–466.
(18) (a) Bailey, W. I., Jr.; Collins, D. M.; Cotton, F. A. *J. Organomet. Chem.* **1977**, *135*, C53–C56. Bailey, W. I., Jr.; Cotton, F. A.; Jamerson, J. D.; Kolb, J. R. *Ibid.* **1976**, *121*, C23–C26. Bailey, W. I., Jr.; Chisholm, M. H.; Cotton, F. A.; Rankel, L. A. *J. Am. Chem. Soc.* **1978**, *100*, 5764–5773. (b) Potenza, J. A.; Johnson, R. J.; Chirico, R.; Efraty, A. *Inorg. Chem.* **1977**, *16*, 2354–2359. (c) Ginley, D. S.; Bock, C. R.; Wrighton, M. S.; Fischer, B.; Tipton, D. L.; Bau, R. *J. Organomet. Chem.* **1978**, *157*, 41–50.
(19) (a) Nicholas, K.; Bray, L. S.; Davis, R. E.; Pettit, R. *J. Chem. Soc., Chem. Commun.* **1971**, 608. (b) Schmitt, H.-J.; Ziegler, M. L. *Z. Naturforsch. B* **1973**, *28*, 508–511.
(20) Nesmeyanov, A. N.; Gusev, A. I.; Pasynskii, A. A.; Anisimov, K. N.; Kolobova, N. E.; Struchkov, Yu. T. *J. Chem. Soc., Chem. Commun.* **1968**, 1365–1366. Gusev, A. I.; Struchkov, Yu. T. *Zh. Strukt. Khim.* **1969**, *10*, 107–115. Gusev, A. I.; Kirillova, N. I.; Struchkov, Yu. T. *Ibid.* **1970**, *11*, 62–70.

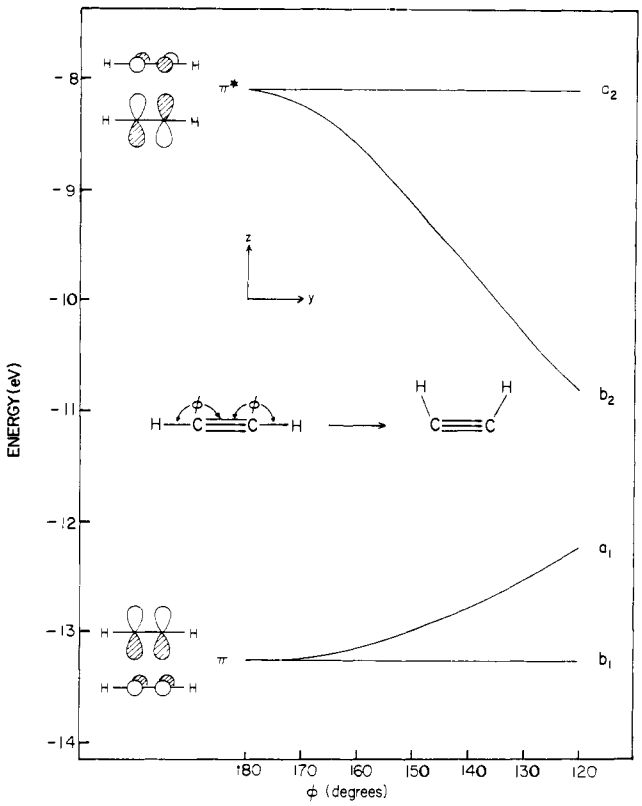

Figure 1. The frontier orbitals of C_2H_2 as the C–C–H angle is varied.

In this contribution we explore the general bonding features of the acetylene complexes, including the question of orientational preference. We use symmetry arguments and extended Hückel calculations in this study. Details relevant to the calculations are provided in the Appendix.

Acetylene MO's

It is apparent from Table I that the acetylene (ac) moiety is affected by its attachment to the dimetal fragment. Free C_2H_2 has a bond length of 1.21 Å while the bridged ac ligands in these complexes show C_{ac}–C_{ac} distances of typically 1.3–1.4 Å. Furthermore, a cis bending away from the normal ac C–C–R angle of 180° is also seen. The parallel-bonded acetylenes have C–C–R angles of 120–130° whereas the range in that angle for the perpendicular orientation is 130–150°.

The Dewar–Chatt–Duncanson model[21] provides a serviceable explanation for the general lengthening of the C_{ac}–C_{ac} bond, but we will have some specific comments to make on the acetylene ligand geometry later. For now it is important that we understand the electronic structure of the distorted acetylene since we will frequently construct the MO's of the ac complexes starting with the orbitals of the ac and L_nMML_n fragments.[22]

In Figure 1 is given the Walsh diagram for the C_2H_2 frontier orbitals, π and π^*. The C–C–H angle is varied from 180° to 120° at a fixed C–C distance of 1.32 Å. Bending at the carbon splits the initially degenerate π and π^* orbitals, producing a four-orbital pattern. The π and π^* orbitals perpendicular to the plane bending, labeled in C_{2v} symmetry and b_1 and a_2, respectively, do not change in energy with bending, because the H's lie in the nodal plane. Orbitals a_1 and b_2, remnants of π and π^*, are affected substantially; a_1 goes up in energy and b_2 comes down. This energy change is a result of mixing of carbon p_y and s into the π and π^* orbital.

(21) (a) Dewar, M. J. S. *Bull. Soc. Chim. Fr.* **1951**, *18*, C71–C79. (b) Chatt, J.; Duncanson, L. A. *J. Chem. Soc.* **1953**, 2939–2947.
(22) For a general reference for acetylene, see: "The Chemistry of the Carbon-Carbon Triple Bond"; Patai, S., Ed.; Wiley: New York, 1978. Early reviews that deal with dinuclear acetylene complexes include the following: Dickson, R. S.; Fraser, P. J. *Adv. Organomet. Chem.* **1974**, *12*, 323–377. Bowden, F. L.; Lever, A. B. P. *Organomet. Chem. Rev.* **1968**, *3*, 227–279.

Table I. Structural Data for Some Selected Acetylene Complexes

complex	distances, Å		angle, deg	ref
	M-M	C_{ac}-C_{ac}	C_{ac}-C_{ac}-R	
	Parallel Orientation			
$Au_2(PPh_3)_2(\mu\text{-}C_2(CF_3)_2)$	3.343 (8)	na[a]	na	1
$Pt_2(CO)_2(PPh_3)_2(\mu\text{-}C_2(CO_2Me)_2)$	2.6354 (8)	1.341 (22)	122.5 (8)	2
$Au_2Me_2(PMe_3)_2(\mu\text{-}C_2(CF_3)_2)$	3.31	1.28	na	3
$Pd_2Cl_2(dpm)_2(\mu\text{-}C_2(CF_3)_2)$[b]	3.492 (1)	1.338 (16)	122.8 (1.1) 124.7 (1.1)	4
$Rh_2Cl_2(dpm)_2(\mu\text{-}C_2(CF_3)_2)$	2.7447 (9)	1.315 (12)	127.4 (9) 128.3 (9)	5
$Rh_2Cl_2(dpm)_2(\mu\text{-}CO)(\mu\text{-}C_2(CO_2Me)_2)$	3.3542 (9)	1.32 (1)	123.8 (4)	6
$Fe_2(CO)_6(\mu\text{-}PPh_2)(\mu\text{-}R^1C_2R^2)$				
$R^1 = P(OEt)_3$ $R^2 = Ph$	2.671 (2)	1.34 (2)	na	7a
$R^1 = CNCMe_3$ $R^2 = Ph$	2.671 (2)	na	na	7b
$R^1 = CN(Me)CH_2CH_2N(Me)$ $R^2 = Ph$	na	1.21 (3)	na	7c
$Fe_2(CO)_8(\mu\text{-}C_6F_4)$	2.797 (1)	1.378 (5)	119.7 (3) 119.3 (3)	8a
$Rh_2(CO)_2Cp_2(\mu\text{-}C_2(CF_3)_2)$	2.682 (1)	1.269 (14)	127.8 (1.1) 129.2 (1.0)	8b
$Rh_2(CO)_2(L_3)(\mu\text{-}C_2(CF_3)_2)$[c]	2.685 (3) A	1.20 (4)	136 (3) 132 (3)	8c
	2.684 (3) B	1.32 (4)	131 (3) 126 (3)	
$Ir_2(CO)_2Cp_2(\mu\text{-}C_6H_4)$	2.7166 (2)	1.386 (3)	119.2 (3) 120.6 (2)	8d
$Fe_2(CO)_6(\mu\text{-}SCF_3)_2(\mu\text{-}C_2(CF_3)_2)$	3.266 (1)	1.34 (1)	na	9
$Ru_2(CO)_4(DAB)(\mu\text{-}C_2H_2)$[d]	2.936 (1)	1.342 (12)	na	10
$Ir_2(NO)_2(PPh_3)_2(\mu\text{-}C_2(CF_3)_2)_2$	na	1.27 (3)[h]	na	11a
$Pt_2(COD)_2(\mu\text{-}C_2(CF_3)_2)_2$[e]	3.129 (2)	1.30 (2) 1.34 (2)	126.5 (17) 125.0 (16) 124.8 (13) 124.8 (10)	11b
	Perpendicular Orientation			
$Ni_2(COD)_2(\mu\text{-}C_2Ph_2)$	2.617 (2)	1.386 (11)	140.6 (4)	12a
$Pt_2(COD)_2(\mu\text{-}PhC_2SiMe_3)$	2.914	1.42 (1)	137.3 (6) Ph 146.4 (6) Si	12b
$Pt_2(C_2Ph_2)(PMe_3)_2(\mu\text{-}C_2Ph_2)$	2.890 (2)	1.36 (5)	na	12c
$Fe_2(CO)_6(\mu\text{-}C_2\text{-}t\text{-}Bu_2)$	2.316 (1)	1.311 (10)	145.3 (6) 144.6 (7)	13a
$Co_2(CO)_6(\mu\text{-}C_2\text{-}t\text{-}Bu_2)$	2.463 (1)	1.335 (6)	144.5 (4) 144.8 (4)	13a
$Co_2(CO)_6(\mu\text{-}C_2Ph_2)$	2.47	1.369	139 137	13b
$Co_2(CO)_4(PPh_3)_2(\mu\text{-}C_2H_2)$	2.464 (1)	1.327 (6)	138	13c
$Co_2(CO)_4(triphos)(\mu\text{-}C_2Ph_2)$[f]	2.512 (3)	1.36 (2)	137.9 (10) 139.7 (10)	13d
$Co_2(CO)_4(dpm)(\mu\text{-}C_2Ph_2)$	2.459 (2)	1.33 (1)	143.2 (9) 137.7 (9)	13e
$Co_2(CO)_2(dam)_2(\mu\text{-}C_2Ph_2)$[g]	2.518 (4)	1.37 (3)	132 (2) 140 (2)	13e
$Co_2(CO)_6(\mu\text{-}C_6F_6)$	2.488 (4)	1.36 (3)	118.6 (1.6) 122.6 (2.0)	13f
$Rh_2(PF_3)_4(PPh_3)_2(\mu\text{-}C_2Ph_2)$	2.740 (1)	1.369 (7)	141.1 (5) 141.5 (5)	13g
$Ir_2(CO)_4(PPh_3)_2(\mu\text{-}HC_2Ph)$	2.691 (1)	1.412 (17)	147.4 (6.4) 137.1 (1.1)	13h
$Co(CO)_3NiCp(\mu\text{-}C_2Ph_2)$	2.3656 (8)	1.337 (5)	144.0 (3) 144.4 (3)	13i
$Ni_2Cp_2(\mu\text{-}C_2H_2)$	2.345 (3)	1.341 (6)	148.1 (5)	13j
$Ni_2Cp_2(\mu\text{-}C_2Ph_2)$	2.329 (4)	1.35 (3)	137.8 (19) 142.0 (19)	13k
$Ni_2Cp_2(\mu\text{-}Ph_2P(O)C_2CF_3)$	2.365 (1)	1.353 (9)	140.7 (6) C 150.2 (5) P	13l
$Pd_2Cp_2(\mu\text{-}C_2Ph_2)$	2.639 (1)	1.33	na	13m
$Rh_2Cp_2(\mu\text{-}CO)(\mu\text{-}C_2(CF_3)_2)$	2.651 (1)	1.363 (8)	137.6 (5) 136.7 (6)	14
$Ta_2Cl_4(THF)_2(\mu\text{-}Cl)_2(\mu\text{-}C_2\text{-}t\text{-}Bu_2)$	2.677 (1)	1.351 (21)	136.26 (64)	15
$Mo_2(O\text{-}i\text{-}Pr)_4(py)_2(\mu\text{-}O\text{-}i\text{-}Pr)_2(\mu\text{-}C_2H_2)$	2.554 (1)	1.368 (6)	na	16
$W_2Br(CO)_5(dam)(\mu\text{-}Br)(\mu\text{-}C_2Me_2)$	2.937 (1)	1.35 (2)	133 (2)[h]	17
$Mo_2(CO)_4Cp_2(\mu\text{-}C_2R_2)$				
R = H	2.980 (1)	1.337 (5)	139 (3) 138 (3)	18a
R = Et	2.977 (1)	1.335 (8)	134.9 (6) 133.4 (6)	18a
R = Ph	2.956 (1)	1.329 (6)	135.4 (4) 133.8 (4)	18a

Table I (*Continued*)

complex	distances, Å M–M	C_{ac}–C_{ac}	angle, deg C_{ac}–C_{ac}–R	ref
$Mo_2(CBD)(CO)_3(\mu\text{-}C_5H_4O)(\mu\text{-}C_2Ph_2)$[i]	2.772 (4)	1.40 (3)	137 (2) 137 (2)	18b
$W_2(CO)_4Cp_2(\mu\text{-}C_2H_2)$	2.987 (1)	1.33 (3)	na	18c
$Fe_2(CO)_4(\mu\text{-}C_2\text{-}t\text{-}Bu_2)_2$	2.215	1.283	142.6 143.0	19a
$Fe_2(CO)_4(\mu\text{-}CC(Me)_2CH_2SCH_2C(Me)_2C)_2$	2.225 (3)	1.272 (20)[h]	139.8 138.7 135.5 141.4	19b
$Nb_2(CO)_2Cp_2(\mu\text{-}C_2R_2)_2$ R = Ph	2.74	1.39	130 129	20
R = CO_2Me	2.732 (5)	1.34 (3)	130 (3) 131 (3)	20

[a] na = not available. [b] dpm = bis(diphenylphosphino)methane. [c] L_3 = dipivaloylmethanato-$CF_3C_2CF_3$. [d] DAB = glyoxal bis(isopropylimine). [e] COD = 1,5-cyclooctadiene. [f] triphos = 1,1,1-tris((diphenylphosphino)methyl)ethane. [g] dam = bis(diphenylarsino)methane. [h] Average. [i] CBD = tetraphenylcyclobutadiene.

The mixing is done in such a way as to hybridize the orbitals away from the H's and from the center of the C_{ac}–C_{ac} axis, **2**. Hy-

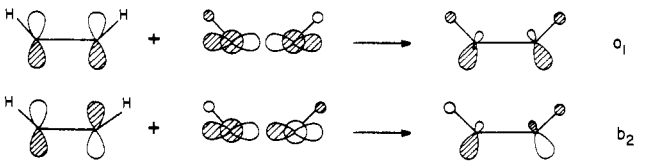

2

bridization lessens the p_z–p_z bonding (a_1) and antibonding (b_2), and so a_1 is destabilized and b_2 stabilized. Just as important as these energy considerations, the hybridization produces lobes beautifully directed for interaction with the L_nMML_n fragment, whether in the parallel or the perpendicular geometry.

The four-orbital pattern of the bent ac is illustrated schematically in **3**. In our analysis we will at times consider both

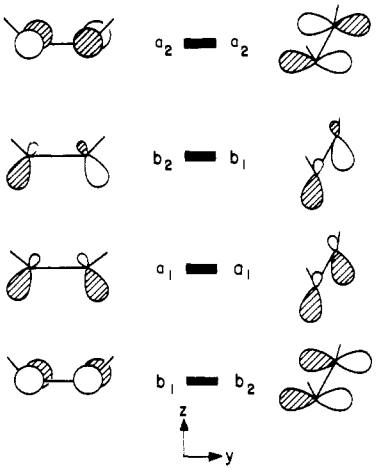

3

orientations of the ac, **1a** and **1b**. Although the known structures of ac complexes range from relatively high symmetry to no symmetry, the M_2C_2 core is pseudo-C_{2v} symmetry, and so we label the orbitals in **3** accordingly.

When we consider both parallel and perpendicular orientations on a L_nMML_n fragment, we choose to turn the ac moiety, keeping the dimetal fragment fixed as in **1**. This arbitrary choice leads to a switching of the b_1 and b_2 symmetry labels of the ac orbitals in **3**. The b_1–b_2 reversal will be important to our analysis.

Before proceeding on to the construction of the acetylene complexes, we must deal with the electron-counting convention. Most chemists, we think, would choose to count ac in the perpendicular configuration as a neutral four-electron donor, two π electrons donated to each metal. The picture would be that of **4a**, with the two lowest orbitals of the acetylene in **3** filled. For

a **4** b

the parallel geometry, we suspect the same chemist would likely count ac as a dianion that still only contributes two electrons to each metal center, **4b**. This requires three orbitals in **3** to be filled, with one noninteracting.

A geometrical problem of concern to us will be the rotation of the acetylene relative to the binuclear framework. In thinking about that motion as a continuous electronic as well as geometric change, it makes sense to keep the electron count the same at all points along a rotation itinerary. A neutral acetylene, perpendicular, parallel, or anywhere in between, is a consistent choice. The tension generated by these two options ((1) ac neutral in the perpendicular geometry, ac^{2-} in the parallel one, vs. (2) ac neutral in both geometries), both rational, is not unhealthy. It makes one aware, not for the first or last time, that any well-defined electron-counting formalism will do, for it is just that, a formalism. We will be very careful to specify our electron-counting assumptions as we proceed.

Let us begin with an analysis of one common perpendicular and one typical parallel acetylene complex type. Then we will delineate the general features of acetylene–metal bonding before returning to a detailed examination of the whole range of available compounds.

A Perpendicular Acetylene Complex

In Table I we list numerous complexes of a general formula M_2L_6(acetylene).[13] We concern ourselves first with those that have a perpendicular ac geometry. All these have structures very similar to $Co_2(CO)_6(\mu\text{-}C_2\text{-}t\text{-}Bu_2)$, **5**.[13a]

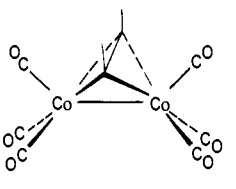

5

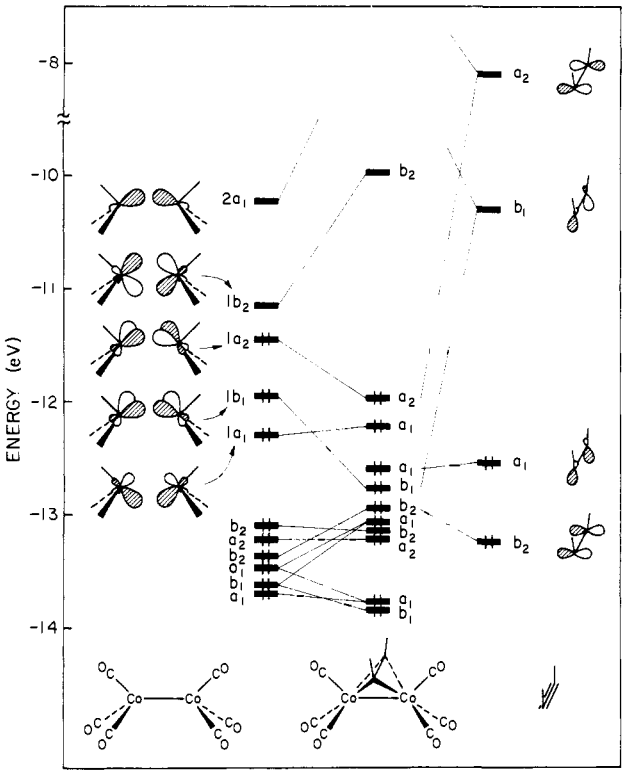

Figure 2. Orbital interaction diagram for $(CO)_3CoCo(CO)_3$ with C_2H_2 in the perpendicular acetylene geometry.

The model system we chose for **5** is $Co_2(CO)_6(C_2H_2)$ with Co–Co = 2.46 Å, C_{ac}–C_{ac} = 1.32 Å, and angle C–C–H = 130°. In Figure 2 we give the interaction diagram for cis bent neutral ac with the $Co_2(CO)_6$ fragment. The orbitals of the dimetal fragment can be easily derived from the individual $Co(CO)_3$ pieces, **6**. This procedure has been described in detail by Thorn and Hoffmann,[23,24] and we repeat only the salient features here.

For the most part the MO's of $Co_2(CO)_6$ are just the in-phase and out-of-phase combinations of the orbitals of $Co(CO)_3$, **6**.

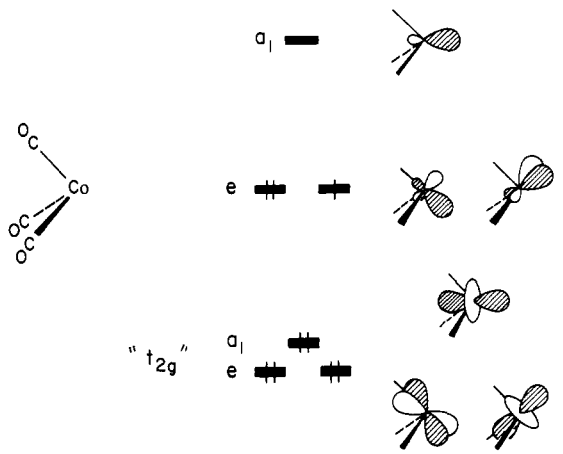

6

Thus there is a low-lying, mainly d, block of six orbitals derived from $1a_1$ and 1e of the mononuclear fragment. Above these are the five valence orbitals $1a_1$, $1b_1$, $1a_2$, $1b_2$, and $2a_1$, derived from 2e and $2a_1$. One orbital, the out-of-phase combination of fragment $2a_1$ levels, is far up in energy and not shown in Figure 2.

The filled orbitals of the bent ac fragment, b_2 and a_1, interact strongly with the empty $Co_2(CO)_6$ orbitals $1b_2$ and $2a_1$, respectively. These interactions are the MO equivalent of the four-electron donor paradigm used for ac in the perpendicular geometry. The empty frontier orbitals of ac, b_1 and a_2, interact very strongly with dimetal fragment filled $1b_1$ and $1a_2$ orbitals. These mixings are identified as the well-known "back-donation". The important interactions just described are shown schematically in **7**.

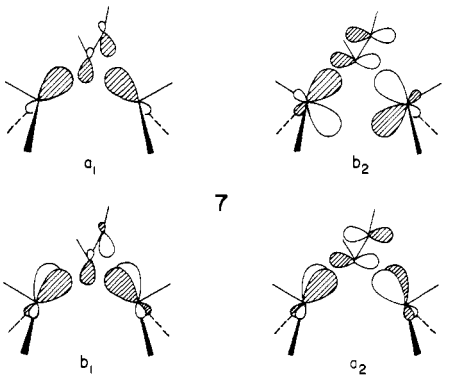

7

The Co–Co overlap population for the composite complex is large and positive, +0.1414, indicating strong Co–Co bonding. It is difficult to isolate in this delocalized MO picture one orbital that is the Co–Co bond. But the $Co_2(CO)_6$ fragment orbital, $1a_1$, essentially nonbonding with the ac fragment, contributes much to the Co–Co overlap population. This "bent" a_1 orbital is similar to the Co–Co bonding orbital described in an ab initio SCF MO calculation on the same molecule.[24b]

We pause here to point out the connection between structures such as **5** and the organic molecule tetrahedrane, **8**. Beneath

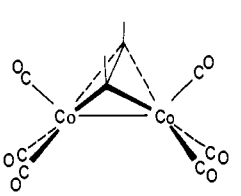

5

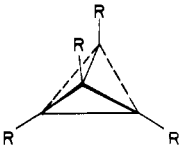

8

the geometrical resemblance lies a profound electronic similarity. The organic CH and the inorganic $Co(CO)_3$ fragments are "isolobal"; i.e., both molecular pieces contain similar but not identical frontier orbitals—in shape, direction in space, approximate energy, and electron count.[25] This relationship will be of importance to us later in this study.

A Parallel Acetylene Complex

Not all $M_2L_6(ac)$ complexes have the acetylene in a perpendicular geometry. Examine $Pd_2Cl_2(dpm)_2(\mu\text{-}C_2(CF_3)_2)$, **9**. The

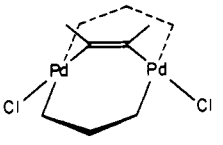

9

acetylene is parallel to the metal–metal axis, but that is not the

(23) Thorn, D. L.; Hoffmann, R. *Inorg. Chem.* **1978**, *17*, 126–140.

(24) Other theoretical studies of dinuclear acetylene complexes include the following: (a) Brown, D. A. *J. Chem. Phys.* **1960**, *33*, 1037–1043. (b) Van Dam, H.; Stufkens, D. J.; Oskan, A.; Doran, M.; Hillier, I. H. *J. Electron Spectrosc. Relat. Phenom.* **1980**, *21*, 47–55. (c) Anderson, A. B. *Inorg. Chem.* **1976**, *15*, 2598–2602; *J. Am. Chem. Soc.* **1978**, *100*, 1153–1159. (d) DeKock, R. L.; Lubben, T. V.; Hwang, J.; Fehlner, T. P. *Ibid.* **1981**, *20*, 1627–1628. (e) Geurts, P.; Burgers, H.; van der Avoird, A. *Chem. Phys.* **1981**, *54*, 397–409. (f) Gavezotti, A.; Ortoleva, E.; Simonetta, M. *J. Chem. Soc., Faraday Trans. 1* **1982**, *78*, 425–436 and references therein.

(25) Elian, M.; Chen, M. M. L.; Mingos, D. M. P.; Hoffmann, R. *Inorg. Chem.* **1976**, *15*, 1148–1155. Albright, T. A.; Hofmann, P.; Hoffmann, R. *J. Am. Chem. Soc.* **1977**, *99*, 7546–7557. Pinhas, A. R.; Albright, T. A.; Hofmann, P.; Hoffmann, R. *Helv. Chim. Acta* **1980**, *63*, 29–49.

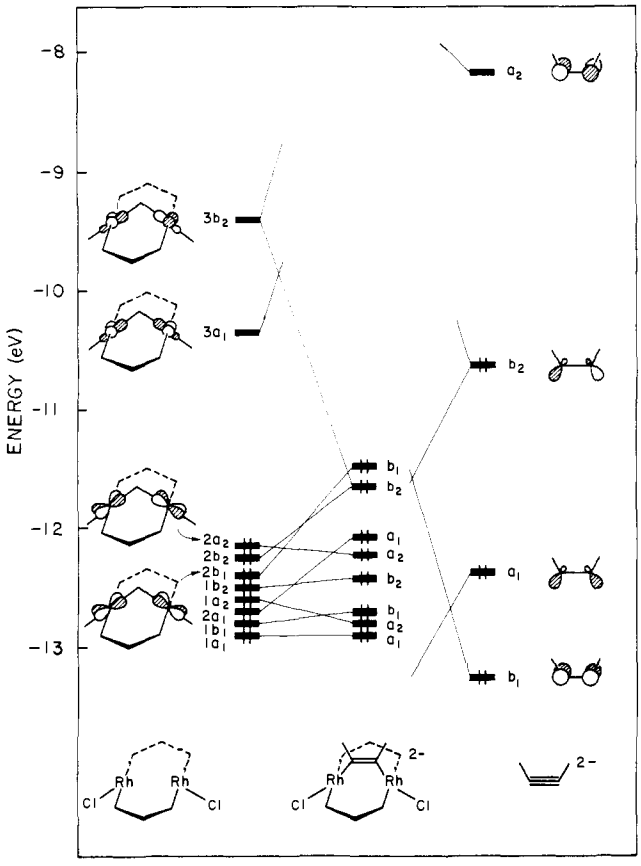

Figure 3. The interaction diagram for $Rh_2Cl_2(dpm')_2$ with $C_2H_2^{2-}$ in the parallel bonding mode. We have assumed Rh–Rh = 3.49 Å and angle C_{ac}–Rh–Cl = 165°.

only structural feature changed. The metal centers are not at all tetrahedral, but approximately square planar, tied by dpm and acetylene bridges. The long Pd–Pd distance is consistent with little or no M–M bonding.[4] The electron count is d^8–d^8 if the acetylene is counted as ac^{2-}, d^9–d^9 if the acetylene is neutral.

Hold in reserve the striking fact that we have two d^9–d^9 complexes (acetylene counted neutral) with very different acetylene orientations *and* metal coordination geometries. Let us first analyze the electronic structure of this complex, something we have actually done in detail elsewhere, in the context of a general study of "A-frames".[26]

In Figure 3 is the interaction of cis bent $C_2H_2^{2-}$ (124°) with d^8–d^8, $Rh_2Cl_2(dpm')_2$ (dpm' = $H_2PCH_2PH_2$) to give $Rh_2Cl_2(dpm')_2(ac)^{2-}$, our model for **9**. The dimetal fragment orbitals are easily derived from two d^8 ML_3 pieces, **10**.[27] The two most

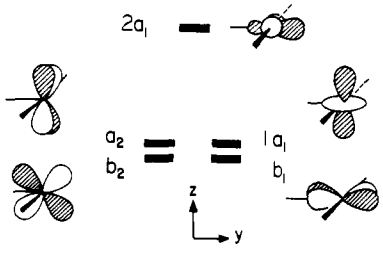

10

important MO's of $Rh_2Cl_2(dpm')_2$ are $3a_1$ and $3b_2$, the in-phase and out-of-phase combinations of the square-planar Rh d orbital that points directly at the bridging ligands. Orbitals $3a_1$ and $3b_2$ lie relatively high in energy, above the third acetylene frontier orbital, b_2. If the acetylene were to be counted as neutral, one of the two orbitals $3a_1$ or $3b_2$ would have to be occupied in what would be a d^9–d^9 dimetal fragment. This is not the only reason to transfer two electrons formally to the acetylene and fill the acetylene π^* derived b_2. By so achieving the d^8 configuration at the two metals, one feels more comfortable about their square-planar environment. There are other reasons to pursue the ac^{2-} formalism for parallel bonded acetylenes that will become clearer later.

The bonding scheme illustrated in Figure 3 is straightforward. Acetylene^{2-} filled b_2 and a_1 interact very nicely with the empty hybrids $3a_1$ and $3b_2$ of the Rh_2 fragment, and the bonding combination resulting from each mixing is filled. Filled b_1 of ac^{2-} mixes most with a filled orbital of the dimetal piece, $2b_1$, and both bonding and antibonding combinations are occupied. The lone acceptor orbital of ac^{2-}, a_2, interacts only slightly with filled $2a_2$ on the dimetal fragment.

As one would expect, the resulting MO scheme for **9** is that of two d^8 square-planar M centers fixed together. The small but important M–M bonding interaction sometimes found for two close d^8 centers is missing here. We find a calculated overlap population of −0.0296, slightly antibonding.[26]

What is the organic analogue of **9**? Is it cyclobutadiene, the isomer of tetrahedrane? No, for several reasons. First the geometry at the metal has changed from local C_{3v} to local C_{2v}, and with that change there comes a major reordering of energy levels. Second, there are no cyclobutadienoid features (for instance, a half-filled near-degenerate level) in the electronic structure of **9**, as shown in Figure 3. The large gap between filled and unfilled levels implies an analogy to a less unsaturated organic molecule.

The isolobal analogy and the lack of M–M bonding supply the clue. A T-shaped C_{2v} d^8 ML_3 fragment is analogous to a d^6 ML_5, which in turn is isolobal with an alkyl cation R^+, **11**. Thus these

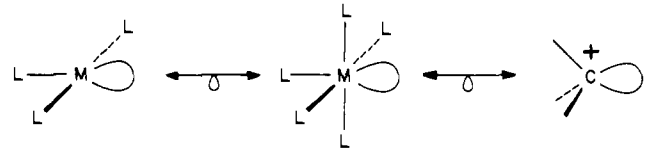

d^8 d^6 **11**

parallel-bonded acetylene complexes are really well described as dimetalated olefins (**12**), an analogy whose full ramifications we will explore in a future contribution.

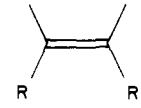

12

From Perpendicular to Parallel

We have seen two complexes with the same metal d electron count (if the acetylene is kept neutral). One has a perpendicular acetylene, the other a parallel one. And while each has the same number of ligands at the metal, aside from the acetylene, the coordination sphere is distinctly different. The obvious question arises: Why is this so? What is wrong with "the other geometry" for each complex, the one obtained by simply twisting the acetylene without modifying the metal coordination?

Taking on this task in stages, we first construct the electronic structure of **13** in Figure 4. The $Co_2(CO)_6$ framework is identical with that in **5**, as is the HC≡CH geometry. Rotating the acetylene around the line joining Co–Co and C–C midpoints gives an unrealistically short metal–carbon distance. So the acetylene moiety has been moved away from the Co–Co vector and adjusted to give the same Co–C distance in **13** as in **5**, 2.0 Å. It is important to note here the change in symmetry labels for the ac fragment orbitals of b symmetry from those in Figure 2, as we described surrounding **3**. Also we ask the reader to refer back to the analysis

(26) Hoffman, D. M.; Hoffmann, R. *Inorg. Chem.* **1981**, *20*, 3543–3555.
(27) For the orbitals of ML_3 and ML_4, see: Albright, T. A.; Hoffmann, R.; Thibeault, J. C.; Thorn, D. L. *J. Am. Chem. Soc.* **1979**, *101*, 3801–3812.

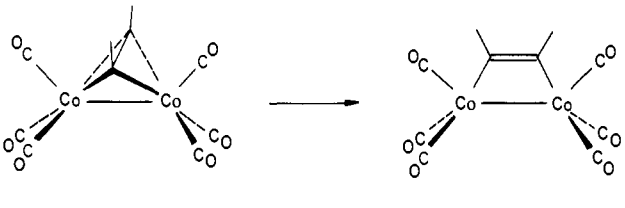

5 13

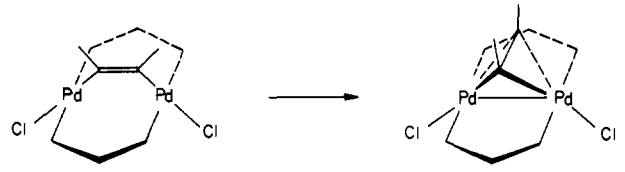

9 14

of Figure 2, for an answer to the geometrical alternative query cannot be given without a detailed comparison of Figures 2 and 4.

There are many differences between **5** and **13**, between Figures 2 and 4. Most are symmetry related. In the parallel configuration, the lowest filled orbital of ac, now b_1, can no longer interact with $1b_2$ and instead mixes with filled $1b_1$, pushing it up. The lowest unfilled orbital of ac, b_2, interacts with empty $1b_2$ and to a lesser extent with a lower filled b_2 orbital. The orbitals of ac of "a" symmetry, a_1 and a_2, do not change symmetry labels on turning. a_1 still interacts strongly with $2a_1$, and now also with $1a_1$. The high-lying a_2, strongly interacting with $1a_2$ in Figure 2, mixes only slightly with the $Co_2(CO)_6$ fragment MO's of a_2 symmetry.

Our extended Hückel calculations give the parallel orientation 2.5 eV above the perpendicular in energy. The preference for the perpendicular geometry is traceable by using the usual perturbational criteria, i.e., overlap and energy match between the interacting orbitals. Upon comparison of Figures 2 and 4, it is evident that the energy match among the orbitals of ac and the important orbitals of $Co_2(CO)_6$, $1a_1$–$2a_1$, is not that different. We look instead to differences in overlap. In **15** are given both

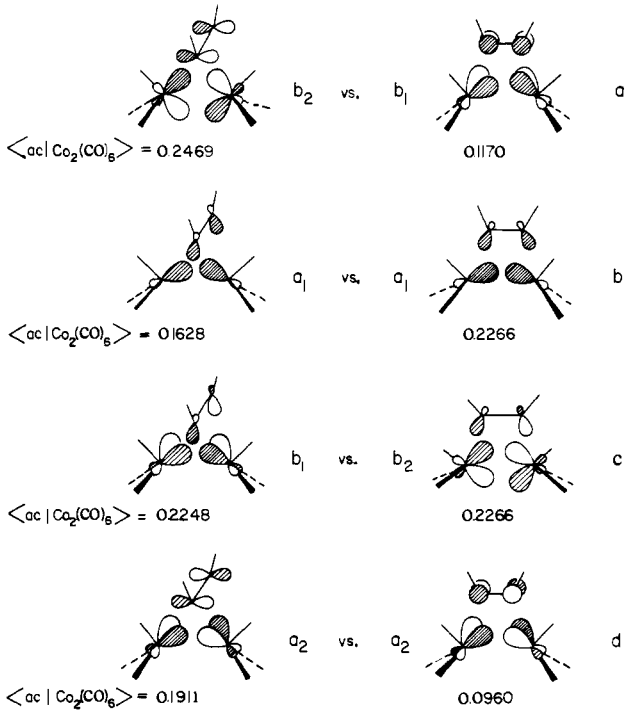

15

schematically and numerically the important overlaps to consider:

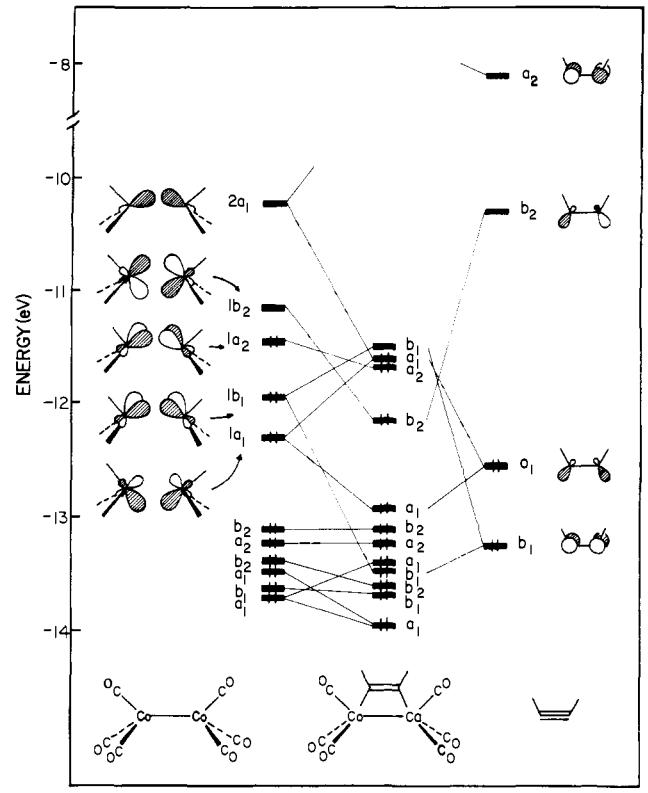

Figure 4. The orbitals of $Co_2(CO)_6(\mu\text{-}C_2H_2)$ in the parallel bonding mode.

15a and **15b** are the overlap between the filled π remnants of ac, and the dimetal fragment and **15c** and **15d** are those involving the π^* remnants of ac. The most notable differences involve the overlaps of the πb orbital of ac and π^*a_2. In both cases the overlap is greater for the perpendicular geometry. This difference in overlap, for the most part, provides the difference in energy between **5** and **13**.

We have chosen to emphasize the disparity in overlap among the various interacting orbitals of ac and $Co_2(CO)_6$ in rationalizing the preference for the perpendicular orientation. Another way of looking at it is to note the four crucial interactions in perpendicular acetylene bonding (see **7**) are all two-orbital two-electron stabilizing interactions. Because of the symmetry label switch of the "b" orbitals, one of the analogous interactions in the parallel geometry becomes a repulsive two-orbital four-electron mixing (ac b_1–$1b_1$), and one becomes a two-orbital no-electron interaction (ac b_2–$1b_2$).

Since a C_{3v} $Co(CO)_3$ is isolobal with CH, the parallel acetylene complex (**13**) should be analogous to cyclobutadiene (**16**). The

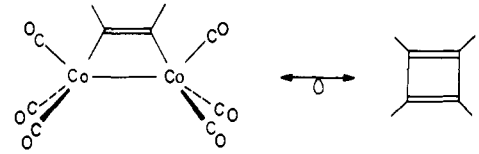

13 16

similarity may be traced in detail. The high-lying and nearly degenerate a_2 and b_1 orbitals of Figure 4 obviously are the counterpart of the nonbonding degenerate π orbitals of a square cyclobutadiene (**17**).

There are several consequences of the cyclobutadiene analogy. First we suspect that a stable system can be attained by the addition of two electrons, occupying the low-lying b_1 LUMO of Figure 4. We do not know of any isolated molecule with the parallel structure of $Co_2(CO)_6(ac)^{2-}$. But the isolobal analogy allows us to see it in the observed structure of $Os_3(CO)_9H_2(C_2R_2)$ (**18a**).[28] When thought of as a diprotonated $Os_3(CO)_9(C_2R_2)^{2-}$,

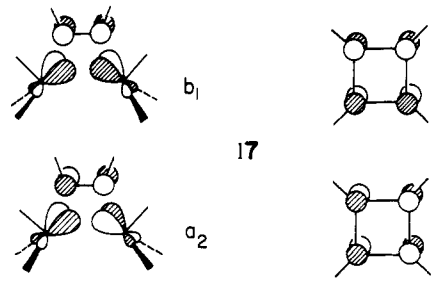

17

this is isolobal with an $Os(CO)_3$ complex of $Os_2(CO)_6(C_2R_2)^{2-}$, which in turn is analogous to an $Fe(CO)_3$ complex of cyclobutadiene. It becomes clear why the acetylene in **18a** is parallel to one edge of the Os_3 triangle.

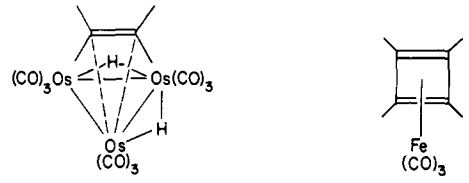

a 18 b

The interconversion of tetrahedrane and cyclobutadiene by a twisting mode, **19**, encounters a level crossing and is said to be

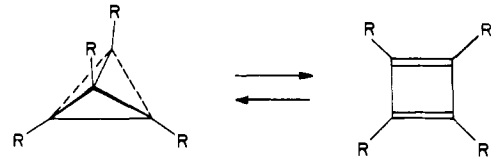

19

symmetry forbidden. There should be a similar problem in the half-inorganic analogue.

We computed a correlation diagram for the rotation **5** → **13**, keeping the $Co-C_{ac}$ distance constant throughout the motion. No barrier was found—**13** simply lies 2.5 eV above **5**. Yet there is a level crossing here, though it is an avoided one. It is between the orbitals shown in **20**. A similar nonessential avoidance of

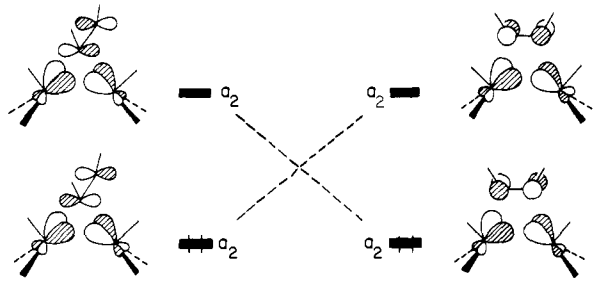

20

a level crossing would be found in the organic analogue, **19**, if two of the four carbons were substituted by heteroatoms. We think it is fair to call the reaction still "forbidden".

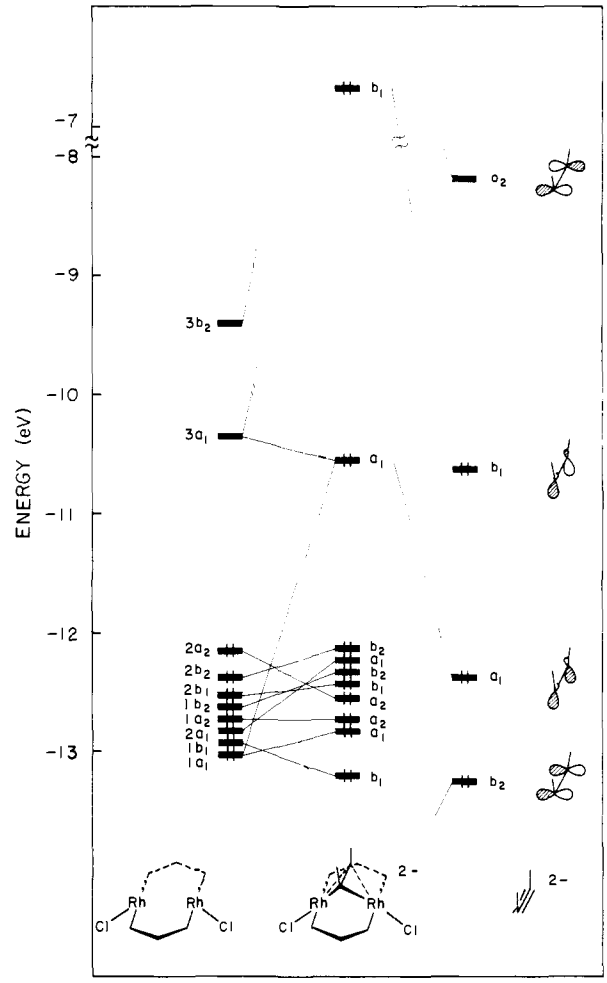

Figure 5. Perpendicular $Rh_2Cl_2(dpm')_2(\mu\text{-}C_2H_2)^{2-}$.

Note Added in Proof: Recent results from McGlinchey and co-workers indicate that a process formally equivalent to rotation of the acetylene in $CpNi(\mu\text{-}PhC_2CO_2\text{-}i\text{-}Pr)Co(CO)_3$ requires $\Delta G^{\ddagger}$ = 20.5 kcal/mol. This is lower than the 2.5-eV barrier we calculate for the isostructural and isolobal model complex $Co_2(CO)_6(\mu\text{-}C_2H_2)$. Calculations on $Co_2Cp(CO)_3(C_2H_2)^-$ and $Co_2Cp_2(C_2H_2)^{2-}$ show that the Cp ligands decrease the barrier to rotation of acetylene to 1.46 and 1.13 eV, respectively. However, the qualitative bonding picture is little changed with substitution of $(CO)_3$ by Cp^-. See ref 49.

We rotated the perpendicular acetylene of a known complex into a parallel orientation and found the process costly in energy. Now we take a known parallel acetylene, **9**, and rotate it into a perpendicular orientation, **14**. The interaction diagram for the much less stable perpendicular $Rh_2Cl_2(dpm')_2(ac)$, Figure 5, is revealing. In the stable parallel orientation the HOMO of ac^{2-} was b_2 and interacted strongly with the empty dimetal fragment $3b_2$. In the perpendicular geometry, the same HOMO is b_1 and can no longer find a symmetry match among the low-lying empty dimetal fragment orbitals. It interacts instead with a filled b_1 below. This four-electron interaction is highly destabilizing, pushing the b_1 antibonding combination to the high energy it has in Figure 5.

The energy we compute for this rotation from parallel to perpendicular is unrealistically high, over 13 eV. No doubt steric effects with the diphosphine bridges exaggerate the magnitude. But given that the parallel complex with locally square-planar ML_3 ends is really isolobal with a disubstituted olefin, it is no surprise that the rotation is costly. The corresponding organic process, **21**, breaks several bonds.

We have now carried out two constrained acetylene rotations without allowing the metal coordination sphere to change. Now it behooves us to attempt the perforce complex composite motion.

(28) Canty, A. J.; Johnson, B. F. G.; Lewis, J. *J. Organomet. Chem.* **1972**, *43*, C35–C38. Canty, A. J.; Domingos, A. J. P.; Johnson, B. F. G.; Lewis, J. *J. Chem. Soc., Dalton Trans.* **1973**, 2056–2061. Deeming, A. J.; Underhill, M. *Ibid.* **1974**, 1415–1419. Deeming, A. J.; Hasso, S.; Underhill, M.; Canty, A. J.; Johnson, B. F. G.; Jackson, W. C.; Lewis, J.; Matheson, T. W. *J. Chem. Soc., Chem. Commun.* **1974**, 807–808. Evans, J.; Johnson, B. F. G.; Lewis, J.; Matheson, T. W. *J. Organomet. Chem.* **1975**, *97*, C16–C18. Humphries, A. P.; Knox, S. A. R. *J. Chem. Soc., Dalton Trans.* **1975**, 1710–1714. Lewis, J.; Johnson, B. F. G. *Pure Appl. Chem.* **1975**, *44*, 43–79. Jackson, W. G.; Johnson, B. F. G.; Lewis, J. *J. Organomet. Chem.* **1977**, *139*, 125–128. Deeming, A. J. *Ibid.* **1978**, *150*, 123–128.

21

It is simpler to do this on a model d^9–d^9 complex (ac neutral), $Co_2H_6(\mu\text{-ac})^{6-}$. The transit examined, **22**, varies simultaneously

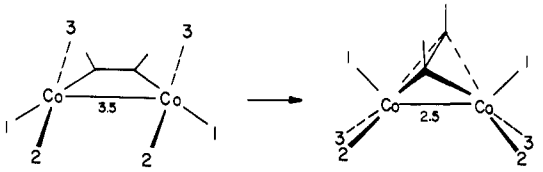

22

the acetylene rotation, the H_2–M–H_3 angle, the Co–Co–H_1 angle, and Co–Co separation, preserving C_2 symmetry. The correlation diagram for this motion shows an explicit level crossing between HOMO and LUMO. This crossing can be traced to an unfilled A-frame a_1 orbital stabilized by the loss of antibonding interaction with the hydrides and a filled b_1 destabilized by an increase in antibonding with the same ligands. This is displayed schematically in **23**. We now see clearly the reasons for the existence of two

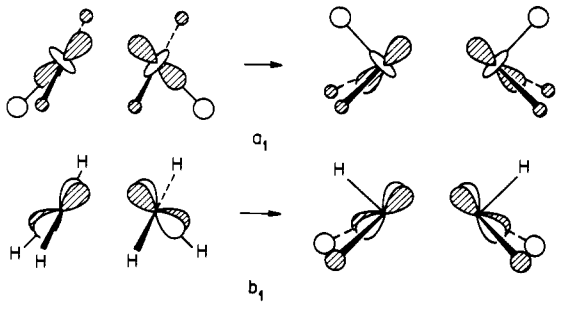

23

separate minima—parallel and perpendicular acetylene, each perforce with different metal coordination geometries.

Two Electrons Less

Acetylene complexes with two less electrons than perpendicular $Co_2(CO)_6(C_2R_2)$ and parallel $Pd_2Cl_2(dpm)_2(C_2R_2)$ exist, e.g., $Fe_2(CO)_6(\mu\text{-}C_2\text{-}t\text{-}Bu_2)$[13a] (**24**) and $Rh_2Cl_2(dpm)_2(C_2(CF_3)_2)$[5] (**25**).

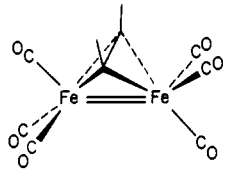

24

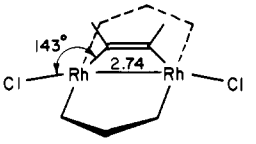

25

The acetylene orientation is maintained, but interesting geometry changes occur.

The Fe_2C_2 core of **24** is similar to Co_2C_2 in **5** except the ac is slightly twisted from perpendicular in **24** by 4–5° and the Fe–Fe distance is significantly shorter, Co–Co = 2.46 Å vs. Fe–Fe = 2.32 Å. The most striking structural difference between **5** and **24**, however, is in the geometry of the $M_2(CO)_6$ units. As shown, **24** has a staggered ethane-type structure whereas **5** is eclipsed. In **25** major structural changes have also occurred. The Rh–Rh bond is substantially shorter and the local metal coordination is best described as distorted trigonal bipyramidal.

The origins of these distortions can be traced to the nature of the vacated orbitals. The pattern of bond-length changes in the series $M_2(CO)_6(C_2\text{-}t\text{-}Bu_2)$, M = Co, Fe,[13a] clearly indicates that in the iron compound an a_2 orbital (**26a**) is vacated.[23,24c] The small

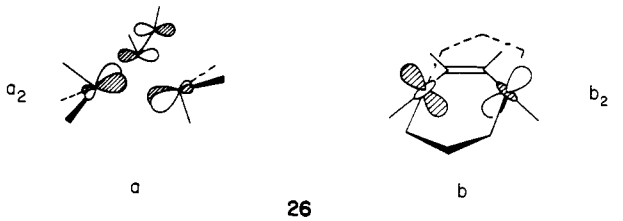

a b

26

HOMO–LUMO gap that might have been expected to result as a consequence (Figure 2) is relieved by twist of the $Fe(CO)_3$ unit. We still think[23,26] that further acetylene twisting may serve a similar purpose.

The orbital that is vacated on going from $M_2Cl_2(dpm)_2(C_2R_2)$, M = Pd to M = Rh, is not the highest-lying b_1 of Figure 3 but the b_2 slightly below it (**26b**). This orbital shoots up in energy as the metal–metal distance decreases, and the deformation of the metal coordination set from locally square planar may be traced to that orbital. For a more detailed analysis, see our construction of the related A-frame SO_2 complex pair.[26]

One of our previous complexes might have benefited from having two electrons removed from it. This was the perpendicular structure obtained by rigid rotation from the known parallel complex, schematically, **27a**. It is clear from Figure 5 that

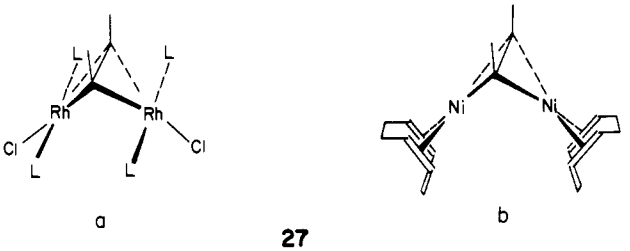

a b

27

vacating b_1 is an excellent idea. The resulting complex can be viewed as a d^8 L_3M("olefin") dimer in the same way that $Ni_2(COD)_2(\mu\text{-}C_2Ph_2)$ (**27b**) has been described as a d^{10} L_2Ni("olefin") dimer.[12a] **27a** represents the dimer of the "wrong" orientation of d^8 L_3M(olefin), **28**. The favored orientation of olefin in d^8

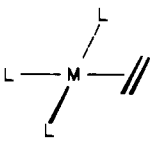

28

L_3M(olefin) complexes, perpendicular to the L_3M plane, is largely due to steric factors.[27] In calculations for **27a** we see orbital interactions that represent steric interactions for a model system with $H_2PCH_2PH_2$ as the bridging ligand.

One Ligand More: M_2L_7(ac) Complexes with a Bridging Ligand

Removing two electrons, as was done in the previous section, creates a hole, a low-lying empty orbital. Geometrical reorganization can and does increase the gap between filled and unfilled levels. A symmetrically placed bridging ligand, as in **29**, ac-

a b

29

complishes the same. In fact, the parallel ac dirhodium complex

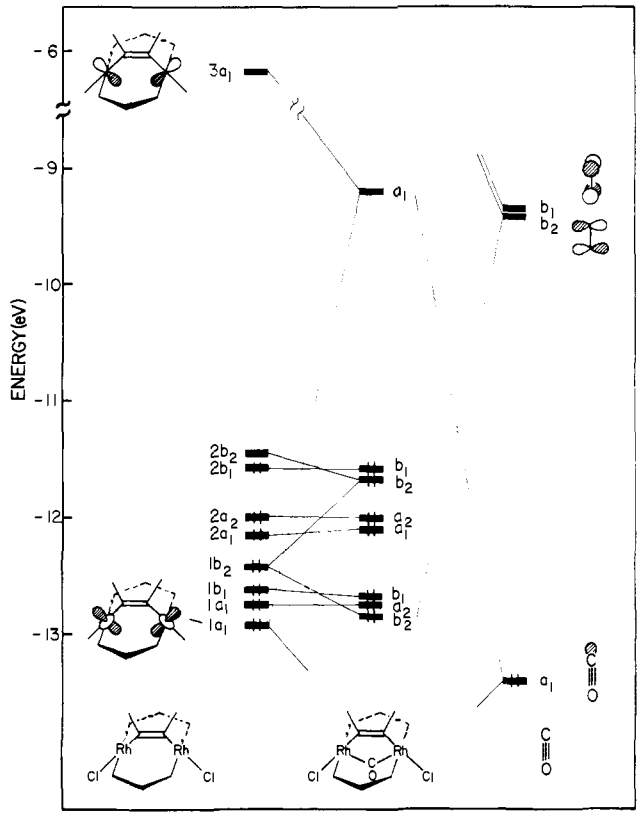

Figure 6. Interaction of neutral CO with the $Rh_2Cl_2(dpm')_2(\mu\text{-}C_2H_2)$ fragment. The Rh–Rh distance is 3.35 Å.

25 reacts with CO to form $Rh_2Cl_2(dpm)_2(\mu\text{-}CO)(\mu\text{-}C_2(CF_3)_2)$ (**30**).[5,6] Upon insertion of CO the Rh–Rh bond length opens

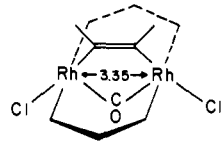

30

considerably from 2.74 to 3.35 Å. Other structural changes occur, and the $Rh_2Cl_2(dpm)_2(ac)$ remnant of **30** that results is structurally similar to the A-frame **9**. Interestingly, the angle at the CO bridge is very large (116°).[6]

It is easy to build up the electronic structure of **30** from the orbitals of $Rh_2Cl_2(dpm')_2(ac)$, which we have seen earlier (Figure 3). This is done in Figure 6. The left side shows that only seven of the eight d block orbitals are filled, consistent with the d^7–d^7 count (ac as ac^{2-}). On the right side are the simple CO orbitals.

The σ lone pair of the CO interacts with the filled $1a_1$ orbital of the Rh_2 d block, the in-phase combination of the two (local) d_{z^2} orbitals of the square-planar Rh centers. The antibonding combination of this mixing is empty and becomes the relatively low-lying LUMO of the molecule, **31**. Its shape suggests the possibility of nucleophilic attack opposite the bridging carbonyl.

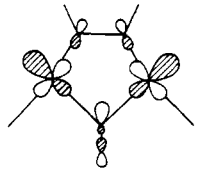

31

As the carbonyl bonds, one of the a_1 orbitals can be thought of as being emptied, and the electrons originally in it transferred to $2b_2$, an empty framework orbital. Recall the discussion of the previous section—it was depopulation of b_2 that made for a short metal–metal bond. Now addition of CO repopulates b_2, and the Rh–Rh bond is once again broken.

Ambiguities concerning the electron count for **30** are not cleared up by our calculations. Counting bridging CO as neutral, one would describe **30** as d^7–d^7. If one counts CO as CO^{2-}, as has been suggested for CO's bridging metal centers without M–M bonding (i.e., large M–CO–M angles), one gets d^6–d^6.[29] Of the lower seven filled MO's for the composite molecule in Figure 6, the upper six are much greater than 50% metal d. The lowest filled orbital shown, b_2, is ~50% d. We do not have any strong feelings about electron-count formalisms. But we do note the electron count of 16 electrons per Rh rationalizes the presence of a low-lying LUMO, **31**. Orbital **31** is the vacant site hybrid of a 16-electron five-coordinate center prepared for takeup of a sixth ligand.

Before we continue, we point out that Figure 6 represents a least motion, or "direct insertion", correlation diagram for a reaction of CO and $Rh_2Cl_2(dpm)_2(ac)$ (**25**) to form **30**. As we discussed above, the b_2 LUMO of **25** is now among the d block in Figure 6. But it should be apparent that it is this orbital that is filled in **30**. Filling the b_2 LUMO of **25** and emptying an a_1 orbital ($1a_1$ in Figure 6) make the least motion path (C_{2v} symmetry) symmetry forbidden. A high barrier is probable, and a pathway where CO attacks one Rh center of **25** first, or a still more complicated non-least motion transit, should be considered.

There also exists an $M_2L_6(\mu\text{-}CO)$ perpendicular acetylene complex of type **29a**, $Rh_2Cp_2(\mu\text{-}CO)(\mu\text{-}C_2(CF_3)_2)$ (**32**).[14] The

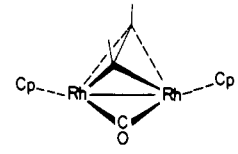

32

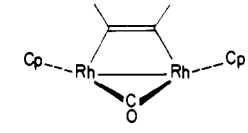

33

Rh–Rh distance in **32** is 2.65 Å, a reasonable Rh–Rh single-bond length. The bridging CO is not directly under the C_{ac}–C_{ac} centroid, and the Cp's are bent back away from the bridging CO. The electron count is d^8–d^8, ac neutral.

Detailed calculations, not presented here, show an electronic structure for **32** not that different from that of $Co_2(CO)_6(ac)$. The M–M bond is slightly weaker in the μ-CO case. Calculations were also done for **33**, the unknown parallel-bonded analogue. **33** is characterized by a rather small HOMO–LUMO separation of approximately 0.5 eV. The LUMO of the parallel structure (**34b**)

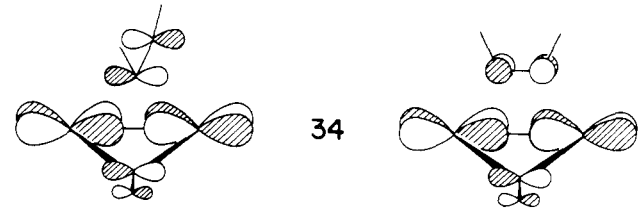

34 a b

resembles the HOMO (**34a**) of the perpendicular complex. It is unoccupied in the parallel complex because the stabilizing mixing of the ac π^* acceptor orbital with the Rh_2 moiety is not as strong as in the perpendicular geometry. The electrons removed from **34a** go partially to ac orbitals, but some of the electron density goes to a Rh–Rh π-type bonding orbital, which is the in-phase version of **34b**. The result is stronger Rh–Rh bonding for the parallel structure.

The calculated total energy for the parallel ac structure **33** was 0.56 eV above that for the known perpendicular geometry **32** (no

(29) Robinson, S. D. *Inorg. Chim. Acta* **1978**, *27*, L108.

optimization). A simple transit to interconvert the two structures, rotation of ac, was examined. The barrier to perpendicular-to-parallel conversion is 1.55 eV. It can be traced to the HOMO, which starts as **34a** in that traverse.

The relatively high calculated barrier for acetylene twisting prevents, at least for this one simple pathway, the interconversion of the two structures. This suggests that the two structures may exist as isomers barring some more complicated interconversion path. One strategy for increasing the viability of structure **33** is to open the HOMO–LUMO gap. This could be accomplished by substituting a π donor at the bridging site for CO. The π donor would mix in antibonding with the metal contribution in **34b** (instead of bonding as CO π^* does), thus pushing the orbital up in energy. A π donor would also destabilize the HOMO of **32** and possibly make structure **33** favored.

Actually we think that **33** is already with us, if not in readily recognizable form. Consider **35a**,[7] **35b**,[30] and some related

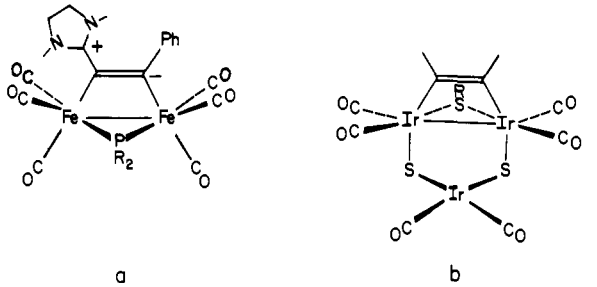

a b

35

structures. Both have π donors at the bridging site and both are d^7–d^7. The $[R_2C^+C^-C^-R]^-$ ligand in **35a** is recognizable as an ac^{2-} equivalent, **36**. The identification for **35b** is simple also if

36

one allows for little or no interaction between the unique Ir and the ac-bridged metals. This is not unreasonable since the Ir···Ir distance is 3.59 Å (average) and the unique Ir is near square planar; i.e., a d^8 count for the unique Ir is appropriate.

General Bonding Features of Bridge-Bonded Acetylenes

We have looked in detail at several known complex types containing both parallel and perpendicular acetylenes. A broader perspective is in order. From our analyses we have gleaned a general picture of bonding of ac with L_nML_n, presented in the interaction diagram of Figure 7.

At right in Figure 7 is ac bonding parallel and at left perpendicular. By now the orbitals of cis bent ac are familiar (**3** and Figure **1**). The schematic L_nML_n orbitals in the center of Figure 7 represent those orbitals important for ac to L_nML_n bonding. As examples, they would model $1b_1$, $1a_2$, $1b_2$, and $2a_1$ in Figure 2 for perpendicular $Co_2(CO)_6$ (ac) or they would correspond to $2b_1$, $2a_2$, $3a_1$ and $3b_2$ in Figure 3 for parallel $Rh_2Cl_2(dpm')_2(ac)^{2-}$. In addition to C_{2v} notation, we label the composite molecule MO's in Figure 7 with a superscript to indicate a parallel ($\parallel$) or a perpendicular ($\perp$) bonding mode.

The bonding schemes presented earlier for $Co_2(CO)_6$ and the $Rh_2Cl_2(dpm')_2$ cases are particularly clear examples of the generalized diagram of Figure 7, and the reader is encouraged to seek out the similarities. Some important features follow.

At left in Figure 7 there are *four* filled $L_nM(ac)ML_n$ MO's that earmark the perpendicular ac to L_nML_n bonding. Two are mainly ac, $a_1^\perp$ and $b_2^\perp$, and two are mainly metal, $b_1^\perp$ and

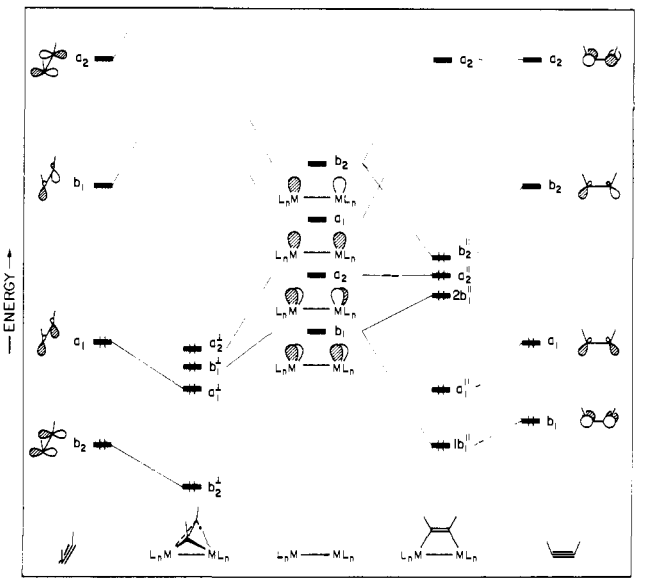

Figure 7. A generalized interaction diagram of the L_nML_n fragment with cis bent C_2H_2. At right is the parallel bonding mode and at left the perpendicular geometry.

$a_2^\perp$. The overlap among the interacting orbitals is good, e.g., **15a–15d**. Both π and both π^* systems of the acetylene are engaged in forward and back donation, respectively.

At right in Figure 7 are the *five* filled MO's that characterize parallel acetylene bonding. Two are of b_1 symmetry. Also there is very little ac π^*a_2–L_nML_n a_2 mixing. These facts reflect the poor ac πb_1–L_nML_n b_1 and ac π^*a_2–L_nML_n a_2 overlap for parallel-bonded ac we have discussed above. Although not obvious from Figure 7, the $b_2^{\parallel}$ orbital will be significantly ac in character. For instance, in Figure 3 ac π^*b_2 falls below the Rh_2 fragment $3b_2$ in energy, and there is good overlap between the orbitals. Much of the ac b_2 is delocalized among the filled b_2 MO's of the composite complex.

The very presence of five low-lying orbitals on the parallel side and four on the perpendicular side is supportive of the different electron-counting scheme, ac (perpendicular) vs. ac^{2-} (parallel), that one is inclined to.

The fragment molecular orbital formalism allows us to analyze the participation of each acetylene orbital in bonding. Table II gives calculated populations of each orbital, as well as some other properties, for several model complexes. Each is based on a *known* ac complex, but the C–C distance is taken as 1.32 Å in all so as to allow the electronic tendencies alone, and not the geometries, to show us the trends.

While there are differences among the various complexes in each group, the dominant feature of this accumulation of data is constancy within each group, parallel or perpendicular, and a dichotomy between the two. Specifically, and consistent with the general analysis of Figure 7, are the following: (1) The ac πb is ~100% occupied in the parallel bonding mode but not in the perpendicular. Similarly, more electrons occupy π^*b in the parallel geometry than in the perpendicular. (2) The ac a_1 occupation is similar in both orientations. (3) The ac π^* a_2 occupation is variable, but, in general, this orbital is little occupied in the parallel geometry.

Now we must face up to the problem of the acetylene ligand neutral or dianionic. The acetylene charge recorded in Table II is relative to a neutral acetylene, whether parallel or perpendicular. As a result of the greater occupation of ac πb and π^*b, the parallel-bonded ac has a net negative charge. The charge on ac for the perpendicular orientation is variable and depends on the π^*a_2 and b_1 back-bonding. In some cases the back-bonding is good enough for the ac charge to rival that of the parallel-bound ac.

So if we begin with the acetylene neutral, the parallel-bonded acetylenes are more negative, overall, than the perpendicular ones.

(30) Devillers, J.; Bonnett, J.-J.; deMontauzon, D.; Galy, J.; Poilblanc, R. *Inorg. Chem.* **1980**, *19*, 154–159.

Table II. Calculational Results for Model Acetylene Complexes

model complex[a]	angle, deg C_{ac}–C_{ac}–H	acetylene orbital occupations[b] πb	πa_1	$\pi^* b$	$\pi^* a_2$	acetylene charge	C_{ac}–C_{ac} OP[c]	ref[d]
Parallel Orientation								
$Au_2(PH_3)_2(\mu\text{-}C_2H_2)$	120	1.98	1.54	1.38	0.03	−0.82	1.3216	1
$Pt_2(CO)_4(\mu\text{-}C_2H_2)$	120	1.96	1.62	1.22	0.04	−0.75	1.3575	2
$Rh_2Cl_2(dpm')_2(\mu\text{-}C_2H_2)^{2-}$	124	2.00	1.49	1.25	0.16	−0.84	1.3334	4
$Rh_2Cl_2(dpm')_2(\mu\text{-}CO)(\mu\text{-}C_2H_2)$	130	1.99	1.46	1.16	0.17	−0.70	1.3508	6
$Fe_2(CO)_8(\mu\text{-}C_2H_2)$	120	2.00	1.44	1.07	0.08	−0.49	1.3826	8a
$Rh_2(CO)_2Cp_2(\mu\text{-}C_2H_2)$	130	1.99	1.57	1.14	0.15	−0.78	1.3641	8b
$Fe_2(CO)_6(\mu\text{-}SH)_2(\mu\text{-}C_2H_2)$	120	1.98	1.38	1.15	0.07	−0.50	1.3792	9
Perpendicular Orientation								
$Pt_2(CO)_4(\mu\text{-}C_2H_2)$	130	1.67	1.80	0.89	0.46	−0.72	1.2137	12a
$Co_2(CO)_6(\mu\text{-}C_2H_2)$	130	1.45	1.79	0.72	0.33	−0.19	1.2498	13a
$Ni_2Cp_2(\mu\text{-}C_2H_2)$	130	1.48	1.77	0.61	0.20	0.11	1.2549	13j
$Rh_2Cp_2(\mu\text{-}CO)(\mu\text{-}C_2H_2)$	130	1.57	1.81	0.86	0.55	−0.69	1.1897	14
$Ta_2Cl_4H_2(\mu\text{-}Cl)_2(\mu\text{-}C_2H_2)^{2-}$	130	1.53	1.68	0.78	0.02	0.13	1.2707	15
$Mo_2Cl_4H_2(\mu\text{-}Cl)_2(\mu\text{-}C_2H_2)^{2-}$	130	1.74	1.77	0.99	0.47	−0.90	1.2093	16
$W_2(CO)_8(\mu\text{-}Cl)(\mu\text{-}C_2H_2)^+$	130	1.37	1.63	0.65	0.27	0.16	1.2523	17

[a] For all model systems C_{ac}–C_{ac} = 1.32 Å. [b] C_{2v} symmetry labels, see 3. [c] OP = overlap population. [d] Reference for real complex upon which model geometry is based. [e] dpm' = $H_2PCH_2PH_2$.

But the full ambiguity of electron counting emerges if we insist on a dianionic acetylene starting point for the parallel-bonded complexes. Then the acetylene loses electron density on complexation, from 1.16 to 1.51 electrons worth, which seems no more realistic than gaining 0.84–0.49 electron, the alternative reference. The ambiguity is there at the orbital level as well—the π^*b orbital, empty in ac and filled in ac^{2-}, has a little more than one electron in it in the complexes studied. Truly the situation is somewhere in between—a problem in electron counting but also an opportunity to see the same molecule from two different electronic sides.

Balch has noted the difficulty in preparing non-acceptor-substituted ac in a parallel geometry.[31] The higher charge on ac found for that orientation may be a partial explanation. However, this cannot be the full answer. For instance, our model for the perpendicular $M_2L_4(ac)$ complexes has a high partial charge on ac, but the actual complexes do not require electron-acceptor-substituted ac.

Taking electrons from filled ac πa_1 and putting them into empty π^*b_2 should cause the acetylene to bend. This follows from the Walsh diagram of Figure 1 and is consistent with ideas about coordinated ligand geometries correlating with excited-state geometries.[32] The parallel-bonded acetylenes have more electrons in π^*b and less in πa_1 than the perpendicular bonded ones. The parallel-bonded ac should then exhibit smaller C–C–R angles (larger bend back angles), and Table I clearly shows this is so.[33]

Another consequence of the ac orbital occupations in Table II is the definite trend we see in C_{ac}–C_{ac} overlap population. The parallel-bonded acetylenes show a larger C_{ac}–C_{ac} overlap population than those bonded perpendicular. The small but significant difference lies in the occupation of the πb and π^*a_2. As we discussed for Figure 1, ac orbitals πa_1 and π^*b lose C_{ac}–C_{ac} bonding and antibonding, respectively, as the C–C–R angle is decreased. Acetylene πb and π^*a_2 are unaffected by the bending (H substitution). The depopulation or population of πb or π^*a_2 is most important in setting the C_{ac}–C_{ac} bond strength. The greater occupation of πb and lesser occupation of π^*a_2 for the parallel configuration when compared to the perpendicular is consistent with the trend in C_{ac}–C_{ac} overlap population observed.

One possible measure of C_{ac}–C_{ac} bond strength is bond length. Careful inspection of Table I shows no clear trend in bond length when those complexes parallel bonded are compared with those perpendicular bonded. Different metals, ligands, and acetylene substituents make direct comparisons difficult. We suggest that as more structures become available, a clear trend toward shorter C_{ac}–C_{ac} bond lengths for parallel-bonded acetylenes will emerge.

We have probed above some structural aspects of the coordinated ac on the basis of the calculated ac orbital occupations. The occupations could in turn be rationalized on the basis of the general interaction diagram in Figure 7 and the MO schemes for actual examples presented here and elsewhere. Let us use Figure 7 again, this time to probe simplistically the question of orientational preference of ac on L_nMML_n.

Assume one has a $L_nM(ac)ML_n$ complex with ac perpendicular bonded; i.e., the left side of Figure 7 applies. If one simply turns ac to parallel bonding (the right side of Figure 7), one is moving uphill in energy. This is because the perpendicular geometry has a more efficient overlap, but only for four orbitals. Furthermore, there are five low-lying orbitals on the right (parallel acetylene side). If only four of these are filled, the system will surely find a distortion to stabilize the molecule. It does so by moving back to the perpendicular geometry.

On the other hand, if one has a closed-shell parallel $L_nM(ac)ML_n$ and turns to the perpendicular geometry, there are too many electrons. Two electrons must go into a high-lying MO of the perpendicular geometry. The deformation will be resisted for five valence electron pairs.

There is another interesting way to apply this general scheme. Let us free ourselves from the constraint of a constant L_nMML_n framework. If a parallel ac complex has a nice closed-shell structure, which perforce leads to a high energy for a corresponding perpendicular isomer, then a related low-energy perpendicular structure can be attained by the equivalent of losing two electrons—kicking out one of the Lewis bases in the metal coordination sphere. It is this concept that is at work in the coexistence of pairs such as in **37**.[34]

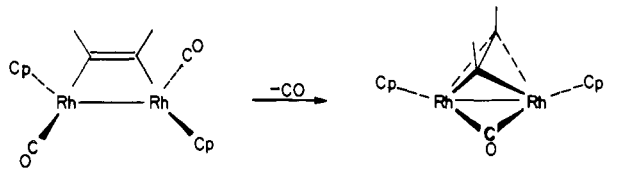

37

The Organic Analogy and Stabilizing Dimetallacyclobutadienes

The isolobal analogy is a remarkable tool—a nonisomorphic mapping of the real complexity of inorganic chemistry on the

(31) Lee, C.-L.; Hunt, C. T.; Balch, A. L. *Inorg. Chem.* **1981**, *20*, 2498–2504.

(32) McWeeny, R.; Mason, R.; Towl, A. D. C. *Faraday Discuss. Chem. Soc.* **1969**, 20–26.

(33) See also: ref 13f. Blizzard, A. C.; Santry, D. P. *J. Am. Chem. Soc.* **1968**, *90*, 5749–5754. Iwashita, Y.; Tamura, F.; Nakamura, A. *Inorg. Chem.* **1969**, *8*, 1179–1183. Iwashita, Y. *Ibid.* **1970**, *9*, 1178–1182. Greaves, E. O.; Lock, C. J. L.; Maitles, P. M. *Can. J. Chem.* **1968**, *46*, 3879–3891.

(34) Dickson, R. S.; Pain, G. N. *J. Chem. Soc., Chem. Commun.* **1979**, 277–278.

apparent simplicity of the organic world. Witness the transformations we have already discussed (**38**). Perpendicular M_2L_6(ac)

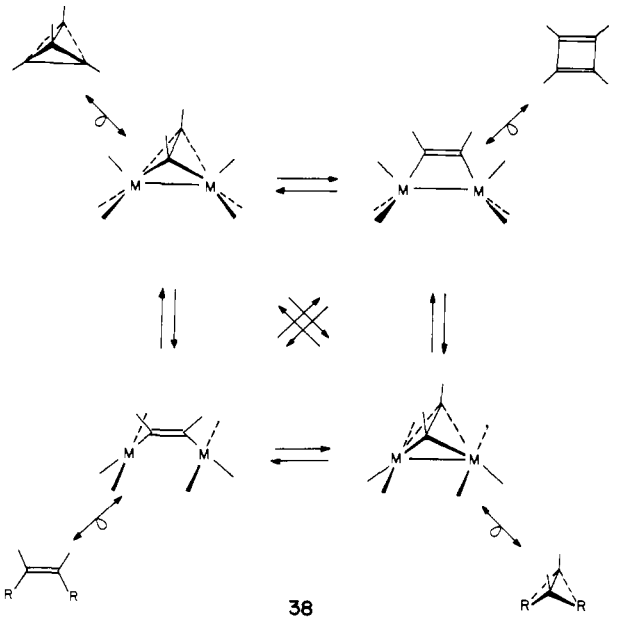

38

complexes with pyramidal d^9 ML_3 groups are like tetrahedrane. Twisted, they become cyclobutadienoid of high energy. They deform the metal coordination sphere to local square planar, losing the metal–metal bond in the process. The isolobal analogy comes over now to an R group or an H atom.

There should be still other local minima on these surfaces. One of these is a dimetallacyclobutadiene (**39**), alternatively a di-

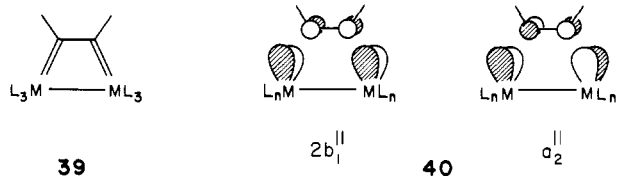

39 **40**

carbenoid structure. The low-lying LUMO for some electron counts in parallel ac complexes brings up a way to think about stabilizing this structure. To get M–C_{ac} π bonding for parallel L_nM(ac)ML_n, one needs to push the $2b_1^{\parallel}$ orbital, **40**, out of the filled MO's of the composite complex while at the same time enhancing the π^* a_2–L_nMML_n interaction, **40**. One way to accomplish this is by choosing an ac substituent that pushes ac πb_1 up in energy while at the same time bringing ac $\pi^* a_2$ down, **41**.

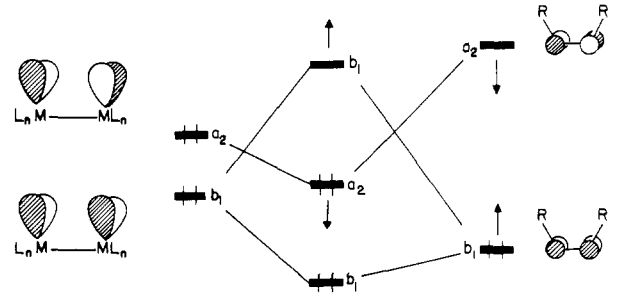

41

For a parallel-bonded species with a low-lying LUMO (e.g., **13**) such a procedure would widen the HOMO–LUMO separation and possibly stabilize the complex.

An acetylene substituent that may accomplish M–C_{ac} π bonding is allyl cation **42**. The allyl cation has a donor orbital of the right symmetry to push ac πb_1 up in energy and an acceptor orbital to push ac $\pi^* a_2$ down (**43**).

There is still another dimetallacyclobutadiene that must be sought. This is **44**, the alternative localized bond structure to **39**.

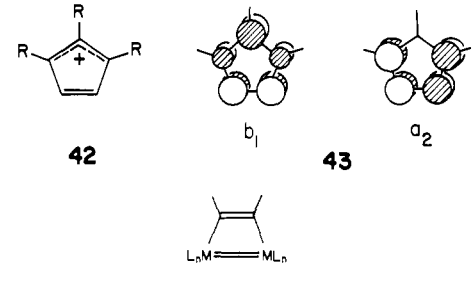

42 **43** **44**

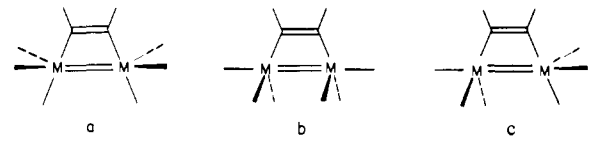

45

Metal–metal multiple bonds at the right side of the transition series are not common, but perhaps with appropriate substituents these complexes can be realized. Their electronic structure and detailed geometry, i.e., **45**, **a**, **b**, or **c**, will be the subject of a separate study.

Acetylene Complexes with a Local Octahedral Geometry at the Metal: Edge-Sharing Octahedra

There are many ac systems we have not yet examined. Some, such as the M_2L_4(ac) and M_2L_2(ac) cases, we take up in separate contributions. We continue here with the ac complexes based upon local octahedral geometry.

In Table I we list four ac complexes that are parallel M_2L_8(ac).[8] Two of these are shown in **46**[8b] and **47**.[8a] Each has ac parallel

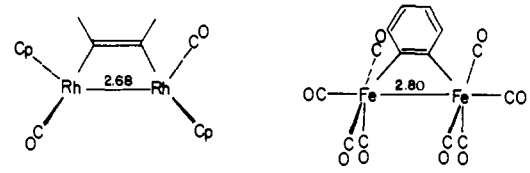

46 **47**

bonded, and the electron count (ac as ac^{2-}) is d^7–d^7. All three have M–M distances suggestive of a M–M bond, as the electron count would dictate.

In Figure 8 we give the interaction diagram for $(CO)_4FeFe(CO)_4^{2+}$ with ac^{2-}. The orbitals of the dinuclear fragment can be derived a number of ways. We prefer to look at it as two d^7 ML_4 pieces. The orbitals of ML_4 have been discussed in detail before,[27] and we simply give them in **48**.

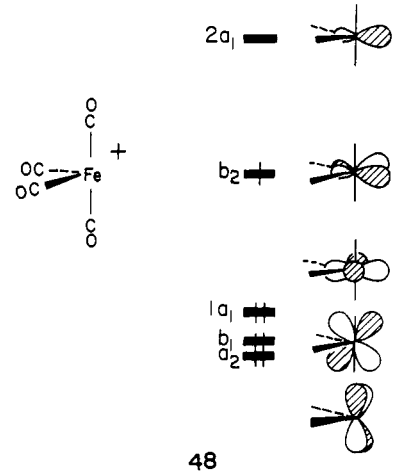

48

The fragment MO's we are most concerned with in the present case are b_2 and $2a_1$. When two d^7 $Fe(CO)_4$ fragments are brought

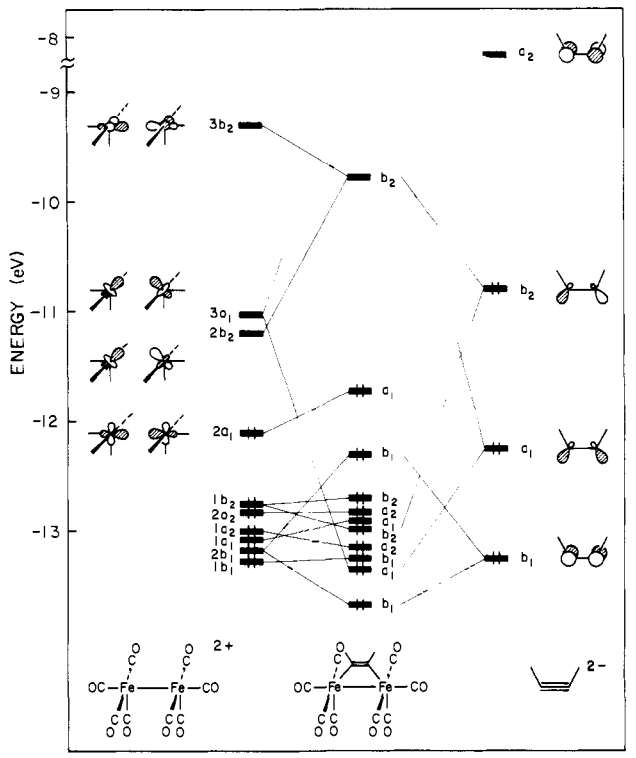

Figure 8. The interaction of $(CO)_4FeFe(CO)_4^{2+}$ with $C_2H_2^{2-}$. The Fe–Fe distance is 2.8 Å and the C_{ac}–C_{ac}–H angle is 120°.

together in a geometry appropriate to **46** and **47**, b_2 and $2a_1$ form four combinations (**49**). The orbitals of the same symmetry mix,

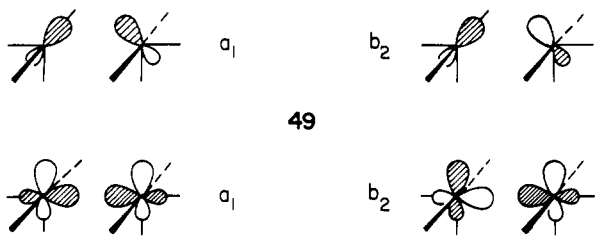

49

but one can identify the upper four orbitals at left in Figure 8, $2a_1$–$3b_2$, as those shown in **49**. For a d^7–d^7 electron count, only one of the combinations is occupied.

The interaction diagram is simple. Filled a_1 and b_2 of ac^{2-} interact strongly with the empty $2b_2$ and $3a_1$ MO's of the Fe_2 fragment. Only the bonding combinations of these mixings are filled, and they represent the Fe–C_{ac} σ bonds. As we discussed in the earlier sections, ac^{2-} b_1 and a_2 do not play an important role in the ac bonding to the dimetal fragment.

The dimetal fragment MO $2a_1$ does not interact very well with the ac and comes over essentially intact in the composite complex (HOMO). This orbital represents the Fe–Fe "bond". Inasmuch as the a_1 HOMO has its orbital density concentrated between the metal centers, one might expect the molecule to be susceptible to attack by small electrophilic ligands at that site. In fact, Dickson and co-workers report[8b] that H^+ reacts with the isoelectronic and isolobal $Rh_2(CO)_2Cp_2(\mu\text{-}C_2(CF_3)_2)$ (**46**), but forms **50** or an alternative but similar structure. We suggest that the initial attack occurs by insertion of the proton into the Rh–Rh bond.

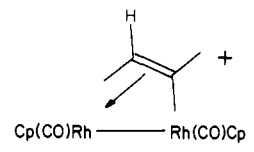

50

The bonding picture described in Figure 8 is similar to that for $Pt_2(CO)_2(PPh_3)_2(\mu\text{-}C_2(CO_2Me)_2)$,[2] (**51**), which we will discuss

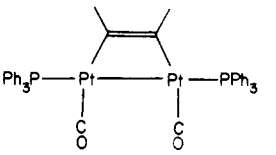

51

in detail in the future. That this must be so is made clear by recalling the isolobal relationship that connects CH_2, d^{10} ML_2, and d^8 ML_4; i.e., both structures **46** (or **47**) and **51** are the inorganic structural analogues to cyclobutene. The relationship between **51** and **46** or **47** is further illustrated by the reactivity exhibited by $Pt_2(COD)_2(\mu\text{-}C_2(CF_3)_2)$, isostructural with **51**. Stone, Green, and co-workers report it reacts with a proton to give **52**, analogous to **50**, going through the cationic Pt(μ-H)Pt hydride.[35]

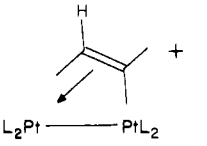

52

The LUMO in Figure 8 is the essentially intact $Fe_2(CO)_8^{2+}$ $3b_2$ orbital. It is strongly antibonding, and filling the orbital should break the M–M bond. Roundhill and Wilkinson[36] proposed some time ago a dicobalt complex, $(CO)_3LCo(ac)CoL(CO)_3$, where L is phosphine or arsine. This is isoelectronic with structural type **46** and **47** but with two electrons more.

We calculated the perpendicular geometry for our model of **46**, **53**, and found it to lie over 4 eV above the known parallel

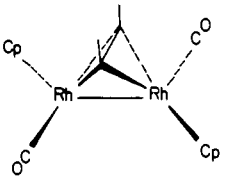

53

geometry. The parallel geometry is favored for the same kind of reasons we discussed in detail for the $M_2L_6(ac)$ A-frame case, Figure 3. The electronic structure of **53** does suggest, however, such a structure might exist with a lower electron count, d^7–d^7 or d^6–d^6.[37]

We consider now the edge-sharing bioctahedral structures with ac at a bridging position. There are two of these, the Fischer complex, $W_2Br(CO)_5(dam)(\mu\text{-}Br)(\mu\text{-}C_2(Me)_2)$ (dam = bis(diphenylarsino)methane) (**54**),[17] and the series of compounds of

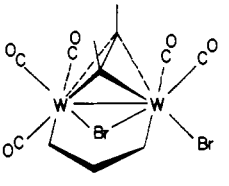

54

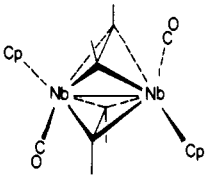

55

Gusev, Pasynskii, Struchkov, and co-workers, $Nb_2(CO)_2Cp_2(\mu\text{-}C_2R_2)_2$, R = Ph, CO_2Me (**55**).[20] Electron counting gives a d^5–d^5

(35) Boag, N. M.; Green, M.; Stone, F. G. A. *J. Chem. Soc., Chem. Commun.* **1980**, 1281–1282.
(36) Roundhill, D. M.; Wilkinson, G. *J. Chem. Soc. A* **1968**, 506–508.
(37) See also: Hofmann, P. *Z. Anal. Chem.* **1980**, *304*, 262–263 and to be published.

count for **54** with a proposed W–W single bond. Structure **55** is d^4–d^4 with the possibility of no bond or a double bond if we adhere to the 18-electron rule. A double bond has been proposed on the basis of the observed diamagnetism of the complex and the short Nb–Nb distance (Table I).[20]

Structures **54** and **55** are related transparently to the common edge-sharing bioctahedral complexes of the $M_2(CO)_8(\mu\text{-}X)_2$ type, **56**. One of us has examined the general class of compounds with

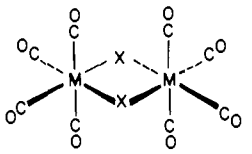

56

structure **56** before, looking at them as a composite of an L_4M ML_4 fragment with a X···X piece.[38] We use the same approach here in order to draw attention to similarities between **54** and **55** and some members of the $L_4M(\mu\text{-}X)_2ML_4$ class.

Both **54** and **55** are low in symmetry, our helpmeet, the first because of its substituent pattern, the latter because of the Cp ligands. We will present in detail our calculations on $Nb_2(CO)_8(ac)_2^{2+}$ (**57**), an isolobal replacement model for **55**. Then

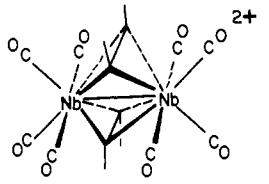

57

we will mention the results of calculations on $Mo_2(CO)_8(\mu\text{-}Cl)(ac)^+$, a model for **54**.

An interaction diagram for $(CO)_4NbNb(CO)_4^{2+}$ and $(ac)_2$ is given in Figure 9. The M_2L_8 fragment orbitals are labeled according to D_{2h} symmetry and σ, π, δ pseudosymmetry. The diacetylene fragment MO's are simply in- and out-of-phase combinations of the four valence MO's. Acetylene–acetylene interactions separate the π and π^* combinations by ~0.5 eV.

The four donor orbitals of the $(ac)_2$ fragment, b_{1u}–b_{3u}, find symmetry and energy matches among the dimetal fragment orbitals. b_{2g} and b_{3u} interact with empty pd hybrids, and b_{1u} mixes with the empty $d_{x^2-z^2}$ out-of-phase combination. The bonding combinations are filled for these mixings. The $(ac)_2$ a_g interaction with the dimetal fragment is more complicated. It interacts with a filled d block MO (in-phase $d_{x^2-z^2}$) and with an empty metal spd hybrid. A three-orbital pattern is the result with the two lowest of the three composite molecule MO's filled ($1a_g$ and $2a_g$).

The empty acceptor orbitals of the $(ac)_2$ interact with their symmetry matches among the filled d block b_{2u}–a_u. It is important that one of the acceptor orbital combinations, b_{3g}, does not interact very much with the $(CO)_4NbNb(CO)_4^{2+}$. The $b_{3g}\pi^*$ orbital of the Nb_2 comes over in the composite complex essentially intact, with only slight mixing from the ac. It lies just above the $2a_g$ and is the LUMO. The orbital is drawn in **58** with overemphasis of the ac contribution.

We label the MO's of the composite complex σ, π, or δ. The considerable ac ligand character of the orbitals makes the assignments difficult. Labeled as they are, the configuration is $\pi^2\delta^2\sigma^2\delta^{*2}$, and so there is a net σ- and π-type double bond. This is somewhat misleading, however, since the "ligand" orbital $2a_g$ has considerable metal character (~40%) and is M–M bonding (**59**). Viewing the complex as double bonded allows us, however, to establish a relationship between **55** and the Vahrenkamp complex, $V_2(CO)_8(PR_2)_2$.[38,39]

(38) Shaik, S.; Hoffmann, R.; Fisel, C. R.; Summerville, R. H. *J. Am. Chem. Soc.* **1980**, *102*, 4555–4572.

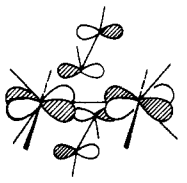

$b_{3g}(\pi^*)$

58

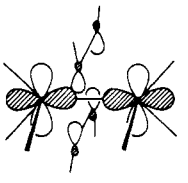

$2a_g$

59

The HOMO–LUMO gap is small for our model calculation (~0.25 eV), and one might be suspicious of the level ordering of b_{3g} above $2a_g$. We did a calculation on a better model, $Nb_2(CO)_2Cp_2(ac)$. The C_{2h} symmetry makes the interaction diagram more complicated, but the orbitals corresponding to $2a_g$ and b_{3g} retain the same order as in Figure 9. We are confident that the b_{3g} (π^*) orbital is above $2a_g$.

A test of the level ordering in Figure 9 would be to force b_{3g} down below $2a_g$ in energy, thereby switching HOMO and LUMO. The HOMO $2a_g$ is M–M and C_{ac}–C_{ac} bonding while b_{3g} is M–M and C_{ac}–C_{ac} antibonding. The change in level ordering should give longer M–M (subject to ac···ac steric constraints) and C_{ac}–C_{ac} distances. Also, the weakened C_{ac}–C_{ac} bond could show enhanced reactivity. One strategy for pushing b_{3g} below $2a_g$ is to substitute acetylene with strong π acceptors and replace the poor π acceptor Cp on Nb with strong π acceptors such as CO.

Structure **55** has an interesting structural distortion we have not mentioned. There is a small twist (~10°) in the same direction of the acetylene ligands relative to the Nb–Nb bond (**60**).

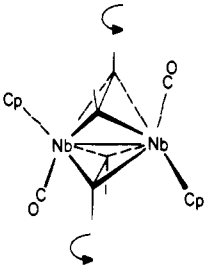

60

The twist has been attributed to steric interactions.[20] There is also a good electronic reason for the twist. In Figure 9, the HOMO and LUMO are close in energy and relatively isolated (as they are in the $Nb_2(CO)_2Cp_2(ac)$ model). Under such conditions, a second-order Jahn–Teller distortion[40] of $a_g \otimes b_{3g} = b_{3g}$ symmetry should be considered. One such distortion is a twist of the acetylenes as in **60**. The model **57** with the acetylenes rigidly rotated by 10° was 0.08 eV lower in energy than the same model with the acetylenes perpendicular.

The small HOMO–LUMO gap also implies the existence of a d^5–d^5 complex.[41] And the $2b_{1u}\sigma^*$ orbital could be filled to give a reasonable d^6–d^6 complex. In both cases the M–M bonding would be weakened. Presumably this effect would manifest itself in longer M–M distances, although the steric constraints of the two ac ligands bumping at longer M–M distances may be a limiting factor in the M–M bond lengths.

(39) Vahrenkamp, H. *Chem. Ber.* **1978**, *111*, 3472–3483.

(40) (a) Den Boer, D. H. W.; Den Boer, P. D.; Longuet-Higgins, H. C. *Mol. Phys.* **1962**, *5*, 387–390. Nicholson, B. J.; Longuet-Higgins, H. C. *Ibid.* **1965**, *9*, 461–472. (b) Bader, R. F. W. *Ibid.* **1960**, *3*, 137–151; *Can. J. Chem.* **1962**, *40*, 1164–1175. (c) Bartell, L. S.; Gavin, R. M., Jr. *J. Chem. Phys.* **1968**, *48*, 2466–2483. (d) Salem, L. *Chem. Phys. Lett.* **1969**, *3*, 99–101. Salem, L.; Wright, J. S. *J. Am. Chem. Soc.* **1969**, *91*, 5947–5955. Salem, L. *Chem. Br.* **1969**, *5*, 449–458. (e) Pearson, R. G. *J. Am. Chem. Soc.* **1969**, *91*, 1252–1254, 4947–4955.

(41) Stone and co-workers have proposed $M_2(CO)_2Cp_2(ac)_2$, M = Cr, Mo, complexes as intermediates in the sequential linking of acetylenes on dichromium and dimolybdenum centers. Knox, S. A. R.; Stansfield, R. F. D.; Stone, F. G. A.; Winter, M. J.; Woodward, P. *J. Chem. Soc., Dalton Trans.* **1982**, 173–185.

We have passed over a calculation on $Mo_2(CO)_8(\mu\text{-}Cl)(ac)^+$, a model for the singly ac bridged **54**. The analysis of this complex is straightforward. The electronic configuration is approximately $\pi^2\delta^{*2}\sigma^2\delta^2\pi^{*2}$ for a net σ bond. So this complex is analogous to the Vahrenkamp $Cr_2(CO)_8(PR_2)_2$.[38,39] There is a relatively low-lying MO that might be filled in a d^6–d^6 compound. Removing two electrons from the model empties a mainly ac ligand type orbital, so what is left may also be termed "d^5–d^5". However, the composition and placement of this orbital are dependent upon the L_4MML_4 ligand set and metal. We do not know if the electrons will come out of the ligand orbital or out of one of the primarily metal MO's.

The unknown d^4–d^4 (ac^{2-}) parallel-bonded complex **61** has a

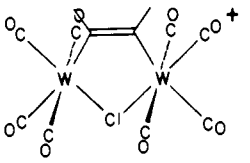

61

low-lying LUMO, and possibly the d^5–d^5 complex will be stable. Electron-count reasoning also suggests a d^6–d^6 species. The EH calculated energy difference for $W_2(CO)_8(\mu\text{-}Cl)(ac)^-$ parallel and perpendicular orientations was 0.3 eV, with the parallel favored (no optimization). However, there are steric problems for structure **61** between the ac and the terminal CO ligands.

A structure that retains the local octahedral environment but avoids the steric interactions in **61** is **62**, a known d^6–d^6 complex

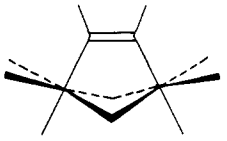

62

in the form of $Fe_2(CO)_6(\mu\text{-}SR)_2(ac)$.[9] Structure **62** is related to some other complexes with the same basic framework, and we will discuss that series in a moment.

Returning to the beautiful $Nb_2(CO)_2Cp_2(ac)_2$ structure, we note that the crystal structure of another diacetylene is known, $Fe_2(CO)_4(\mu\text{-}C_2\text{-}t\text{-}Bu_2)_2$ (**63**).[19] The Fe–Fe distance is extremely short,

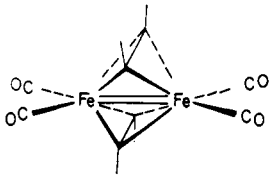

63

2.215 Å, and on the basis of it, the observed diamagnetism, and electron counting, Pettit and co-workers proposed an Fe–Fe double bond.[19a] The orbitals of the $d^8M(CO)_2$ and $(ac)_2$ moieties in hand, the construction of the MO scheme for this complex is not difficult. We do not detail the procedure here. We do point out our calculations reveal two low-lying empty orbitals for structure **63**. They are drawn schematically in **64**.

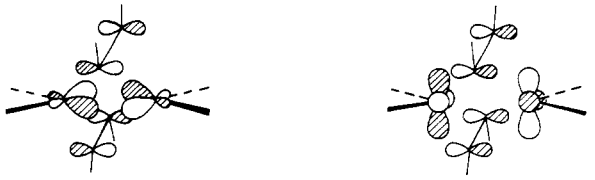

a b

64

It does not seem unreasonable to suppose one could fill either or both of the orbitals, weakening the M–M bonding. M_2L_6 d^{10}–d^{10} tetrahedral dimers are known (**65**), but most complexes

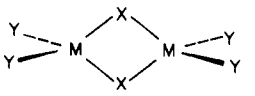

65

of structural type **65** have d^8–d^8 (e.g., **63**) or d^9–d^9 counts. The mixed-metal complex **66** (M = Mo, W) recently synthesized by Davidson is "half" of the d^9–d^9 diacetylene structure.[42]

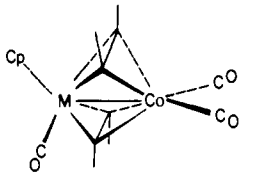

66

Interestingly, $M_2L_4(ac)_2$ complexes do exist with four more electrons than **63**. They are $Ir_2(NO)_2(PR_3)_2(\mu\text{-}C_2(CF_3)_2)_2$[11a] and the related $Pt_2(COD)_2(\mu\text{-}C_2(CF_3)_2)_2$.[11b] But both acetylenes in these complexes are parallel bonded, and the M centers are near square planar (**67**). A d^8–d^8 count is appropriate. The structural

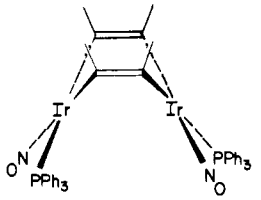

67

dichotomy of the $M_2L_4(ac)_2$ complexes, **63** vs. **67**, is tied up with the alternative structures available to the general class of M_2L_6 complexes, the tetrahedral dimer **65** and the square planar dimer **68**. But that is another story.[43]

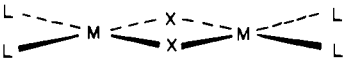

68

Face-Sharing Bioctahedral Complexes

We now turn to another type of binuclear acetylene complex based on a face-sharing bioctahedral geometry, $L_3M(\mu\text{-}L)_2(ac)\text{-}ML_3$. We know of three examples whose crystal structures have been determined: $Fe_2(CO)_6(\mu\text{-}SCF_3)_2(\mu\text{-}C_2(CF_3)_2)$,[9] $Ta_2Cl_4(\mu\text{-}Cl)_2(THF)_2(\mu\text{-}C_2Me_2)$,[15] and $Mo_2(O\text{-}i\text{-}Pr)_4(\mu\text{-}O\text{-}i\text{-}Pr)_2(py)_2(\mu\text{-}C_2H_2)$,[16] **69**, **70**, and **71**, respectively. Electron-counting pro-

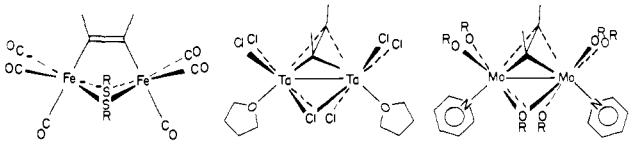

69 70 71

cedures would suggest different M–M interactions for **69**–**71**. Structure **69** is d^6–d^6, and one would not suppose Fe–Fe bonding, nor does the Fe–Fe distance of 3.27 Å suggest any. The Ta(III) complex **70** has a short Ta–Ta distance of 2.68 Å, and Cotton

(42) Davidson, J. L.; Manojlovic-Muir, K. W.; Keith, A. N. *J. Chem. Soc., Chem. Commun.* **1980**, 749–750.
(43) Summerville, R. H.; Hoffmann, R. *J. Am. Chem. Soc.* **1976**, *98*, 7240–7254.

has proposed a double bond.[15] Chisholm and co-workers relate that the Mo–Mo distance in the Mo(III) complex **71** is 2.55 Å, consistent with a Mo–Mo single bond.

In order to make the derivation of the MO schemes for **69–71** more tractable, we chose to start with the electronic structure of the well-known $L_3M(\mu\text{-}X)_3ML_3$ series where X = π donor.[44] The acetylene ligand is then viewed as a perturbation to the MO's of the more symmetrical structure **72**.

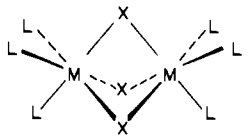

72

The "t_{2g}" combinations of the local octahedral centers of structure **72** are the orbitals we need to consider. They are drawn schematically in **73**. We do not mean to imply any level ordering

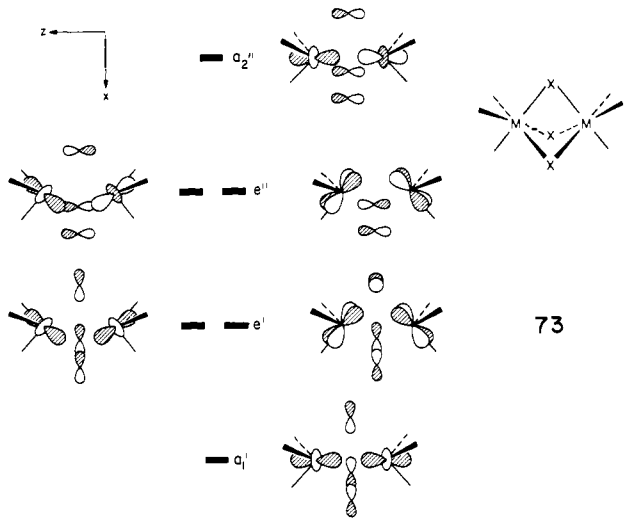

73

in **73**. The energy of the MO's is dependent upon the ligand set and M–ligand and M–M interaction.[44]

We begin with the simplest case, the Fe_2 complex **69**. All six d-block orbitals (**73**) are filled in this complex. The actual bonding of the acetylene to the Fe_2 moiety is through orbitals not shown in **73**, the "e_g" combinations **74a** and **74b**. These are the σ M–C_{ac}

a b

74

bonds. They are also M–M bonding and antibonding, respectively. Because of a better energy match between the ac π^* and the out-of-phase metal combination, **74b** will contain a higher metal contribution than **74a**. Thus, the M–M interaction will be overall antibonding.

It is interesting that a d^7–d^7 species, $Rh_2Cp_2(\mu\text{-}CO)_2(C_2(CF_3)_2)$ (**75**), has been proposed as one form of **46** in solution. One empty

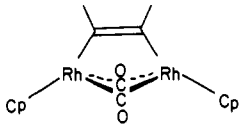

75

(44) See: Summerville, R. H.; Hoffmann, R. *J. Am. Chem. Soc.* **1979**, *101*, 3821–3831 and references therein.

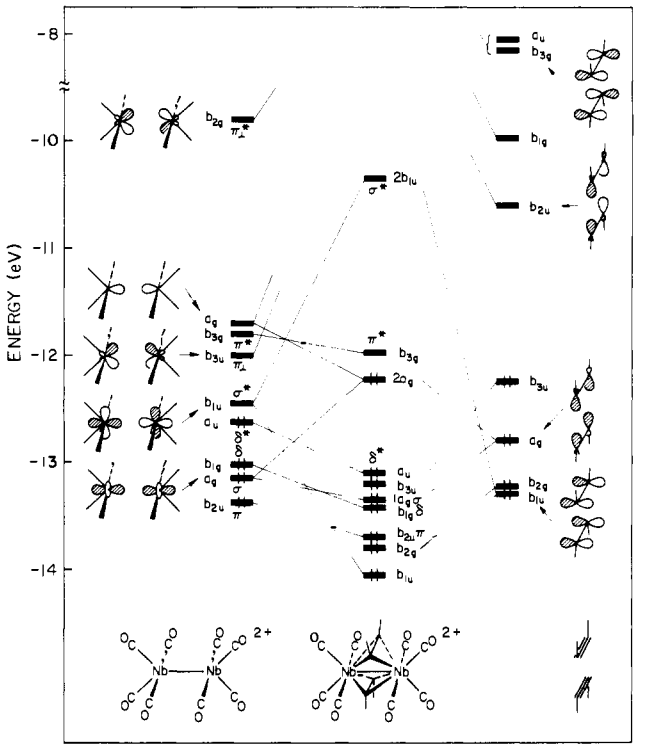

Figure 9. Orbital interaction diagram for $(C_2H_2\cdots C_2H_2)$ with $(CO)_4NbNb(CO)_4^{2+}$. We have assumed Nb–Nb = 2.74 Å and Nb–C_{ac} = 2.24 Å.

orbital of **69** is **76a**. As shown, the π-donor bridging ligand mixes into this orbital antibonding. The π-acceptor CO groups would mix in a bonding way (**76b**) and drive the orbital down in energy. It is **76b** that is occupied by the two extra electrons for the d^7–d^7 complex.

a b

76

Let us consider the ac in its perpendicular orientation, **70** and **71**. For **70** and **71**, the level ordering is crucial, and the ac will have a pronounced effect. The orbitals in **73** mainly affected by the substitution of one μ-X by perpendicular ac are those that interact with the acceptor π^* ac orbitals, one member each of e′ and e″. The interaction with the ac π^* orbitals is bonding (**77** and **78**) and forces the orbitals down in energy.

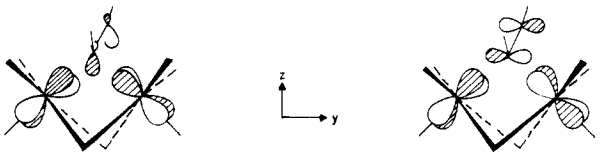

b_1 a_2

77 **78**

We did calculations on the model complexes $Ta_2Cl_4(\mu\text{-}Cl)_2H_2(C_2H_2)^{2-}$ and $Mo_2Cl_4(\mu\text{-}Cl)_2H_2(C_2H_2)^{2-}$, isoelectronic with **70** and **71**, respectively. The hydrides modeled the presumably innocent THF and pyridine ligands. The MO schemes are complicated by considerable ac mixing into the MO's of the complexes. However, for both cases we obtain **77**, b_1 in C_{2v} symmetry, the lowest occupied MO that is reasonably considered metal "d". Near it in energy are two orbitals, mainly ac π, that we call "ligand"

Table III. Parameters Used in Extended Hückel Calculations

orbital	H_{ii}, eV	ζ_1	ζ_2	C_1[a]	C_2[a]
P 3s	−18.60	1.60			
3p	−14.00	1.60			
S 3s	−20.00	1.817			
3p	−13.30	1.817			
Cl 3s	−30.00	2.033			
3p	−15.00	2.033			
Au 5d	−15.07	6.163	2.794	0.6851	0.5696
6s	−10.92	2.602			
6p	−5.55	2.584			
Co 3d	−13.18	5.55	2.10	0.5679	0.6059
4s	−9.21	2.00			
4p	−5.29	2.00			
Fe 3d	−12.60	5.35	2.00	0.5505	0.6260
4s	−9.10	1.90			
4p	−5.32	1.90			
Mo 4d	−10.50	4.54	1.90	0.6097	0.6097
5s	−8.34	1.96			
5p	−5.24	1.92			
Nb 4d	−12.10	4.08	1.64	0.6401	0.5516
5s	−10.10	1.89			
5p	−6.86	1.85			
Ni 3d	−12.99	5.79	2.00	0.5683	0.6292
4s	−8.86	2.10			
4p	−4.90	2.10			
Pt 5d	−12.59	6.013	2.696	0.6334	0.5513
6s	−9.077	2.554			
6p	−5.475	2.554			
Rh 4d	−12.91	4.29	1.97	0.5807	0.5685
5s	−9.26	2.135			
5p	−3.88	2.10			
Rh 4d	−12.50	4.29	1.97	0.5807	0.5685
5s	−8.09	2.135			
5p	−4.57	2.10			
Ta 5d	−12.10	4.762	1.938	0.6815	0.5774
6s	−10.10	2.28			
6p	−6.86	2.241			
W 5d	−10.37	4.982	2.068	0.6940	0.5631
6s	−8.26	2.341			
6p	−5.17	2.309			

[a] These are the coefficients in the double-ζ expansion.

orbitals. These two orbitals have amounts of metal character ranging with the M–M distance and ligand set. Above these three orbitals is an a_1 (C_{2v}) orbital (**79**) most resembling a_1' in **73**.

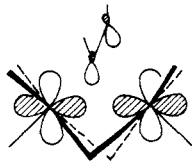

a_1

79

Orbital **79** has considerable M–M bonding character. Above a_1 lies a_2 (**78**).

For the d^2–d^2 Ta_2 complex **70**, b_1 and a_1 (**77** and **79**) are occupied and a_2 (**78**) is the low-lying LUMO. Adding two more electrons occupies a_2, and this orbital is the HOMO for **71**. If we precariously label the filled MO's of **70** and **71** by the σ, π, and δ designation, we have a ($\pi^2\sigma^2$) configuration for **70** and a ($\pi^2\sigma^2\pi^{*2}$) configuration for **71**. As is obvious from our schematic drawing of the orbitals in **77** and **78**, the distinction between π and δ is muddled. Even **79** will have some π character.

The orbitals **77**–**79** suggest there is a handle on the level ordering. One might be able to force a_2 (**78**) below a_1 (**79**) by substituting ac with a π acceptor. If the electron count were d^2–d^2, one would have a $\pi^2\pi^{*2}$ configuration (if closed shell), and presumably the M–M distance would stretch.

We could not have looked at each of the known dinuclear acetylene complexes individually. We did examine what we consider to be a representative sampling. Some classes, such as $M_2L_4(ac)$ and $M_2L_2(ac)$, we consider separately. The important Mo and W $M_2L_{10}(ac)$ complexes, for example, **80**,[18] have been

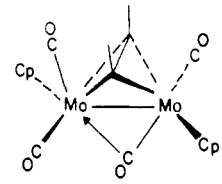

80

analyzed elsewhere.[37] We save for future contributions the incredibly diverse reaction chemistry exhibited by dinuclear acetylene complexes.

Acknowledgment. Support for this work came from the National Science Foundation in three ways: through Research Grant CHE 7828048, through the Cornell Materials Science Grant DMR 7681083, and through the Undergraduate Research Grant program which supported C.R.F. We are grateful to S. Chester for the skillfully rendered drawings and to E. Stolz and L. Stout for the typing.

Appendix

All calculations were performed with the extended Hückel method,[45] with weighted H_{ij}'s.[46] Reasonable geometries were assumed for the model calculations and based upon the known complexes when possible. For rotation of ac on the L_nML_n fragment, the M–C_{ac} distance was fixed for each point of the transit. Bond distances used throughout include C_{ac}–C_{ac}, 1.32 Å; C–H, 1.09 Å; P–H, 1.44 Å; M–H, 1.7 Å; C–O, 1.16 Å.

The parameters used in our calculations are listed in Table III. The parameters for C, N, O, and H are the standard ones.[45] All metal parameters are from previous publications,[26,27,43,47] except for Ta metal exponents from Basch and Gray.[48]

Registry No. $Au_2(PH_3)_2(\mu\text{-}C_2H_2)$, 81830-96-8; $Pt_25(CO)_4(\mu\text{-}C_2H_2)$, 81830-97-9; $Rh_2Cl_2(dpm')_2(\mu\text{-}C_2H_2)$, 81830-98-0; $Rh_2Cl_2(dpm')_2(\mu\text{-}CO)(\mu\text{-}C_2H_2)$, 81830-99-1; $Fe_2(CO)_8(\mu\text{-}C_2H_2)$, 81831-00-7; $Rh_2(CO)_2Cp_2(\mu\text{-}C_2H_2)$, 81831-01-8; $Fe_2(CO)_6(\mu\text{-}SH)_2(\mu\text{-}C_2H_2)$, 81846-84-6; $Pt_2(CO)_4(\mu\text{-}C_2H_2)$, 81846-85-7; $Co_2(CO)_6(\mu\text{-}C_2H_2)$, 12264-05-0; $Ni_2Cp_2(\mu\text{-}C_2H_2)$, 52445-55-3; $Rh_2Cp_2(\mu\text{-}CO)(\mu\text{-}C_2H_2)$, 81831-02-9; $Ta_2Cl_4H_2(\mu\text{-}Cl)_2(\mu\text{-}C_2H_2)^{2-}$, 81831-03-0; $Mo_2Cl_4H_2(\mu\text{-}Cl)_2(\mu\text{-}C_2H_2)^{2-}$, 81831-04-1; $W_2(CO)_8(\mu\text{-}Cl)(\mu\text{-}C_2H_2)^+$, 81831-05-2.

(45) Hoffmann, R. *J. Chem. Phys.* **1963**, *39*, 1397–1412. Hoffmann, R.; Lipscomb, W. N. *Ibid.* **1962**, *36*, 2179–2195; **1962**, *37*, 2872–2883.
(46) Ammeter, J. H.; Burgi, H. B.; Thibeault, J. C.; Hoffmann, R. *J. Am. Chem. Soc.* **1978**, *100*, 3686–3692.
(47) Komiya, S.; Albright, T. A.; Hoffmann, R.; Kochi, J. K. *J. Am. Chem. Soc.* **1976**, *98*, 7255–7265. Dedieu, A.; Albright, T. A.; Hoffmann, R. *Ibid.* **1979**, *101*, 3141–3151. Goddard, R. J.; Hoffmann, R.; Jemmis, E. D. *Ibid.* **1980**, *102*, 7667–7676.
(48) Basch, H.; Gray, H. B. *Theor. Chim. Acta* **1966**, *4*, 367–376.
(49) Jaouen, G.; Marinetti, A.; Saillard, J.-Y.; Sayer, B. G.; McGlinchey, M. J. *Organometallics* **1982**, *1*, 225–227.